Hindawi Publishing Corporation
Journal of Computational Engineering
Volume 2014, Article ID 501590, 18 pages
http://dx.doi.org/10.1155/2014/501590

Research Article

Shape of Slender Axisymmetric Ventilated Supercavities

Igor Nesteruk

Institute of Hydromechanics, National Academy of Sciences of Ukraine, Zhelyabova 8/4, Kyiv 03680, Ukraine

Correspondence should be addressed to Igor Nesteruk; inesteruk@yahoo.com

Received 29 November 2013; Accepted 27 January 2014; Published 23 March 2014

Academic Editor: Fu-Yun Zhao

Copyright © 2014 Igor Nesteruk. This is an open access article distributed under the Creative Commons Attribution License, which permits unrestricted use, distribution, and reproduction in any medium, provided the original work is properly cited.

The integral-differential equation was obtained to simulate unsteady evolutions of the slender axisymmetric ventilated supercavity with the use of one-dimensional inviscid flow of the incompressible gas in the channel between the cavity surface and the body of revolution. For small ventilation rates, the solution of this equation was expressed as asymptotic series. In the steady case the nonlinear differential equation and its solutions were obtained. It was shown that the ventilation can increase and diminish the supercavity dimensions. Examples of calculations for different hull shapes are presented. At some critical values of the gas injection rate the cavity dimensions can become unbounded. Stability of steady and pulsating gas cavities was investigated in the case of the low gas injection rate.

1. Introduction

The drag of high speed underwater vehicles can be reduced with the use of supercavitation. This idea was developed in many theoretical, numerical, and experimental investigations in a lot of countries. In 2013 we celebrated the 100 anniversary of the famous Ukrainian academician G. V. Logvinovich who sufficiently contributed to both the theoretical and experimental research of supercavitation and practical applications of this phenomenon. His principle of independence (Logvinovich [1]) is still the very efficient tool for calculating the shape of long 3D cavities. In this paper we will discuss its accuracy and areas of application.

To obtain small cavitation numbers at small vehicle velocities or at large movement depths, a gas ventilation inside the cavity is used (see, e.g., Logvinovich [1], Epshtein [2–4], Knapp et al. [5], Yegorov et al. [6], Levkovsky [7], Kuklinski et al. [8], Spurk [9], Wosnik et al. [10], Zhuravlev and Varyukhin [11], Matveev et al. [12], and Vlasenko and Savchenko [13]). In most cases the gas and vapor densities inside the cavity are much smaller than the density of water (approximately 800 times). This fact allows neglecting the influence of the gas flow inside the cavity and assuming the constant pressure on its surface. As a result, in the case of small gravity effects, the cavitation number

$$\sigma_0 = \frac{2\left(p_\infty - p_0 - p_v\right)}{\rho U_\infty^2} \tag{1}$$

(ρ is the water density, U_∞ is the velocity of movement, p_v is the water vapor pressure at ambient temperature, and p_∞ and p_0 are pressures measured in the cross section of the cavity origin far away in the water flow and in the injected gas, resp.) is supposed to be constant over all of the cavity surface and the ventilated cavity shape is assumed to be coinciding with the vapor one. This fact is usually used both in theories of the ventilated cavities (e.g., Logvinovich [1], Epshtein [2–4], and Spurk [9]) and in experiments. For example, in tests by Wosnik et al. [10] and Vlasenko and Savchenko [13] the pressure inside the ventilated cavity was not measured, but the shape of the corresponding vapor cavity was used to estimate the cavitation number. Even in this case, when the effects of the gas flow inside the cavity and gravity are negligible, there is no complete theory for the cavity shape as a function of the gas supply rate, cavitation number, and the shape of the body located inside the cavity.

To improve the efficiency of the supercavitation in comparison with the attached flow pattern, the cavitation number has to be reduced and the cavity volume has to be used completely to locate the vehicle hull (see, e.g., Nesteruk [14]). It means that an injected gas must flow in a narrow channel between the cavity surface and the vehicle hull; see Figure 1. If the ventilation rate is large enough, the pressure on the cavity surface is no more constant and changes the cavity shape in comparison with the case of vapor cavitation. This complicated phenomenon could be investigated numerically

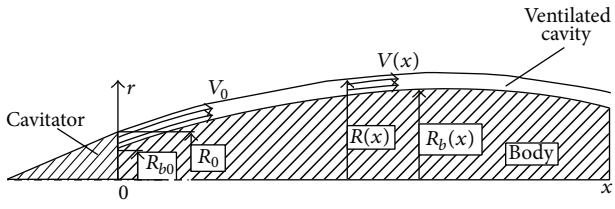

Figure 1: Axisymmetric supercavitation flow pattern with the gas ventilation in a circular channel between the vehicle hull and the cavity at the initial moment of time $t = 0$.

with the use of viscous fluid equations (e.g., Zhuravlev and Varyukhin [11]). The ideal fluid approach and the slender body theory allow one to obtain simple equations for the shape of axisymmetric ventilated supercavity provided that the gas flow between the cavity surface and the body of revolution is one-dimensional inviscid and incompressible. Some interesting results were obtained in Manova et al. [15] and Nesteruk and Shepetyuk [16, 17] for steady flow of liquid without gravity effects.

Here the results of these papers are generalized for the unsteady vertical flows in the gravity field. The integral-differential equation is obtained to simulate unsteady evolutions of the slender axisymmetric ventilated supercavity. For small ventilation rates, a solution is expressed as asymptotic series. Examples of the steady cavity shape calculations for different hulls are presented. Peculiarities of the cavity closing near the hull contour discontinuities were investigated.

Stability and pulsations of ventilated cavities were investigated experimentally in Silberman and Song [18], Song [19], Michel [20], and Zou et al. [21] and by many other authors. The theories of such empty cavities were proposed by Woods [22], Paryshev [23, 24], Nesteruk [25], and Semenenko [26]. Here we will try to construct simple stability theories for the steady and pulsating cavities with the use of the main term of the developed asymptotic solution. In comparison with the previous investigations we will take into account cases of the hull, located inside the cavity, different cavitator shapes, and the influence of the gravity.

2. Slender Body of Revolution with a Prescribed Pressure Distribution

The theory of supercavitation is very complicated due to the absence of exact solutions for 3D unsteady flows even in ideal fluid. But for long cavities similar to the slender bodies of revolution, the corresponding linear theories can be used. In monograph (Cole [27]) the potential of the steady flow of ideal incompressible liquid was obtained by the method of matched asymptotic expansions. In Nesteruk [28], this slender body theory was generalized for the unsteady case. The potential of the external water flow can be written as follows:

$$\begin{aligned}\Phi(x,r,t,\varepsilon) &= x + \varepsilon^2 \ln \varepsilon A(x,t) \\ &\quad + \varepsilon^2 \{A(x,t)\ln r_* + B(x,t)\} + O\left(\varepsilon^4 \ln \varepsilon\right);\end{aligned} \tag{2}$$

$$\varepsilon = \frac{R'_{\max}}{L'}; \qquad r_* = \frac{r}{\varepsilon};$$

$$A(x,t) = F(x,t)\left(\frac{\partial F}{\partial x} + \tau \frac{\partial F}{\partial t}\right); \tag{3}$$

$$F(x,t) = \frac{R(x,t)}{\varepsilon};$$

$$\Phi(x,r,t) = \frac{\Phi'(x,r,t)}{L' U'_\infty(t)}; \qquad \tau(t) = \frac{L'}{t'_x U'_\infty(t)}; \tag{4}$$

$$t = \frac{t'}{t'_x};$$

$$\begin{aligned}B(x,t) = &-A(x,t)\ln 2 \\ &- \frac{1}{2}\int \frac{\partial A(\xi,t)}{\partial \xi} \operatorname{sign}(x-\xi) \ln|x-\xi|\, d\xi.\end{aligned} \tag{5}$$

We use the symbols with "prime" for physical (dimensional) parameters; t'_x is the typical time of unsteadiness, for example, the pulsation period; $R(x,t) = R'(x,t)/L'$ is the body or the cavity radius; ε is a small parameter, a ratio of the maximum radius of the body $R'_{\max}$ (or a cavitator-cavity system) to its length L' at a fixed moment of time t; x, r are cylindrical coordinates shown in Figure 1; the integration in (5) must be carried out along the axis of symmetry from the nose till the tail of the body. If the body shape $R(x,t)$ and the function $U'_\infty(t)$ are known, (2)–(5) allow one to calculate the flow field and the pressure distribution.

In supercavitating flows (or when the body shape is unknown), the radius $R(x,t)$ may be calculated with the use of pressure distribution $p'(x,t)$ over the surface. Putting expression (2) into the Cauchy-Lagrange integral yields (Nesteruk [28, 29])

$$\begin{aligned}&\varepsilon^2 \ln \varepsilon Z(A) + \varepsilon^2 \left[Z(A)\ln F + Z(B) + 0.5A^2F^{-2}\right] \\ &\quad + O\left(\varepsilon^4 \ln^2 \varepsilon\right) = -0.5C_p(x,t) \pm x\mathrm{Fr}^{-2}(t),\end{aligned} \tag{6}$$

$$Z(U) \equiv \tau \frac{\partial U}{\partial t} + \frac{\partial U}{\partial x} + SU;$$

$$S(t) = \frac{L'}{\left(U'_\infty\right)^2}\frac{dU'_\infty}{dt'}; \qquad \mathrm{Fr}(t) = \frac{U'_\infty(t)}{\sqrt{gL'}}, \tag{7}$$

$$C_p(x,t) \equiv \frac{2\left[p'(x,t) - p'_\infty(0,t)\right]}{\rho U'^2_\infty(t)}. \tag{8}$$

Here $\mathrm{Fr}(t)$ is the Froude number, g is the gravity acceleration, and $p'_\infty(0,t)$ is pressure in liquid far from the body at the level $x = 0$. The sign "–" in the last term of (6) corresponds to the gravitational acceleration vector directed along the x axis and the sign "+" corresponds to the case, when the directions of the body movement and gravity coincide (in order to have an axisymmetric cavity the direction of the gravity force is limited by these two cases). The dimensionless speeds are based on the current flow velocity $U'_\infty(t)$.

Nonlinear integral-differential equation (6) relates the slender body (or the cavity) radius and the pressure distribution in liquid over its surface $p'(x,t)$. If the functions $p'(x,t)$, $p'_\infty(0,t)$, and $U'_\infty(t)$ and the cavitator shape are given, the set of (3)–(8) allows one to calculate the unknown cavity radius $R(x,t)$. The asymptotic solution of the nonlinear integral-differential equation (6) was obtained in Nesteruk [30].

3. Equation of the First Approximation and Logvinovich's Principle of Independence

The leading term of (6) (of order $\varepsilon^2 \ln \varepsilon$) provides the equation of the first approximation (Nesteruk [28]):

$$\varepsilon^2 \ln \varepsilon \left[\tau \frac{\partial A}{\partial t} + \frac{\partial A}{\partial x} + SA \right] = \pm x \mathrm{Fr}^{-2}(t) - 0.5 C_p(x,t). \tag{9}$$

Thus the squared body (or cavity) radius can be found by successive integration of two linear differential equations (9) and (3) with partial derivatives of the first order. The corresponding general solution was obtained in Nesteruk [28].

Equation (9) can be rewritten in the absolute coordinates x_a, r_a (in which the liquid at infinity does not move and the body moves vertically). Let us suppose that the origin of this coordinate system is located on the undisturbed free water surface; the directions of the axis of symmetry x_a and the cavitator movement are opposite and the pressure $p'_c(t)$ on the cavity surface depends on the time only. Then (9) attains the following form (Nesteruk [30]):

$$\ln \varepsilon \frac{\partial^2 R^2}{\partial t^2} = \sigma_{\mathrm{at}}(t) \pm \frac{2x_a}{\mathrm{Fr}_0^2}, \tag{10}$$

$$\sigma_{\mathrm{at}}(t) = \frac{2\left[p'_{\mathrm{at}} - p'_c(t)\right]}{\rho U'^2_\infty(t_0)}, \qquad \mathrm{Fr}_0 = \frac{U'_\infty(t_0)}{\sqrt{gL'}}, \qquad t'_x = \frac{L'}{U'_\infty(t_0)}, \tag{11}$$

where t_0 is some fixed moment of time and the atmospheric pressure p'_{at} on the undisturbed free water surface is assumed to be constant. The thickness parameter ε can be assumed to be coinciding with the ratio of the cavitator maximum radius to its length, for example, for slender conical cavitator $\varepsilon = \beta = tg(\theta)$ (2θ is the cone angle).

According to (10), the evolution of every cross section of the cavity (at fixed value of x_a) is independent of the cavity behavior at other cross sections. This fact can be considered as one more theoretical support of Logvinovich's principle of independence. An equation similar to (10) with an empirical constant instead of $\ln \varepsilon$ is used in the computer codes developed in the Institute of Hydromechanics NASU for the calculations of unsteady supercavities, for example, Semenenko and Naumova [31].

It must be noted that the accuracy of the first approximation (9) or (10) is limited by value $|\ln \varepsilon|^{-1}$, which yields only 44% for $\varepsilon = 0.1$ and 22% for $\varepsilon = 0.01$. However these equations provide a nice qualitative description and were used to estimate the influence of many physical parameters such as gravity, capillarity, liquid compressibility, the cavitator shape, motion unsteadiness, and pressure gradients over the body surface; see Nesteruk [28–30, 32–34]. To improve the accuracy, the integral-differential equation (6) must be used, in which the independence of the cavity cross section is no more valid due to the integral term (5).

4. Shape of the Ventilated Axisymmetric Slender Cavity

In the case of ventilated cavity the total pressure of the water vapor and the gas $p_v + p_g(x,t)$ must be equal to the pressure in water on the cavity surface $p_c(x,t)$. Here we neglect the capillarity forces and use the approach of one-dimensional flow of an ideal incompressible gas in the circular channel between the cavity surface and the hull located inside the cavity (see Figure 1). Then the continuity equation yields that the gas flux

$$Q(t) = \frac{Q'(t)}{(L')^2 U'_\infty(t)} = \pi V(x,t) W(x,t); \qquad W(x,t) = R^2(x,t) - R_b^2(x,t) \tag{12}$$

inside the cavity is only time dependent. Here the dimensionless gas velocity $V(x,t)$ is based on $U'_\infty(t)$; the dimensionless cavity and body radii ($R(x,t)$ and $R_b(x,t)$) are based on L'. By neglecting the longitudinal curvature of the circular channel (the body inside the cavity is assumed to be slender too), the potential of the one-dimensional gas flow can be determined from the relationship

$$V(x,t) = \frac{\partial \Phi_g(x,t)}{\partial x}, \qquad \Phi_g(x,r,t) = \frac{\Phi'_g(x,r,t)}{L' U'_\infty(t)} \tag{13}$$

and (12) as follows:

$$\Phi_g(x,t) = \frac{Q(t)}{\pi} \int_0^x \frac{dx}{W(x,t)} + \phi_1(t), \tag{14}$$

where $\phi_1(t)$ is an arbitrary time dependent function.

The Cauchy-Lagrange integral for the gas flow has the following form:

$$\frac{\partial \Phi'_g}{\partial t'} + \frac{(V')^2}{2} + \frac{p'_g}{\rho'_g} = \left[\frac{\partial \Phi'_g}{\partial t'} + \frac{(V')^2}{2} + \frac{p'_g}{\rho'_g} \right]_{x=0}, \tag{15}$$

where ρ'_g is the gas density. Gravity and inertial forces are neglected in (15), since $\rho'/\rho'_g \approx 800$ and they are very much smaller in comparison with the same forces in water flow,

taken into account in (6). Putting expressions (12) and (14) into (15) yields

$$\begin{aligned} C_p(x,t) &= \frac{2\left[p_c'(x,t) - p_\infty'(0,t)\right]}{\rho' U_\infty'^2(t)} \\ &= \frac{2\left[p_g'(x,t) + p_v - p_\infty'(0,t)\right]}{\rho' U_\infty'^2(t)} \\ &= -\frac{2\rho_g'\tau(t)}{\pi\rho'}\frac{\partial}{\partial t}\left[Q(t)\int_0^x \frac{dx}{W(x,t)}\right] \\ &\quad - \sigma_0(t) + \frac{\rho_g' Q^2(t)}{\rho'\pi^2}\left[W^{-2}(0,t) - W^{-2}(x,t)\right] \\ &\quad - \frac{2\rho_g' Q(t) S(t)}{\pi\rho'}\int_0^x \frac{dx}{W(x,t)}. \end{aligned} \tag{16}$$

Here $R_0(t) = R(0,t)$ and $R_{b0}(t) = R_b(0,t)$ are the radii of the cavity and the body at the cross section of cavity origin $x = 0$ (see Figure 1); the cavitator and body shapes can be changeable; $\sigma_0(t)$ is given by (1). Substitution of (16) into (6) yields the following nonlinear integral-differential equation for the ventilated cavity shape:

$$\begin{aligned} &\varepsilon^2 \ln\varepsilon Z(A) + \varepsilon^2\left[Z(A)\ln F + Z(B) + 0.5A^2F^{-2}\right] \\ &\quad + O\left(\varepsilon^4\ln^2\varepsilon\right) = 0.5\sigma_0(t) \pm x\mathrm{Fr}^{-2}(t) \\ &\quad + \frac{\rho_g\tau(t)}{\pi\rho}\frac{\partial}{\partial t}\left[Q(t)\int_0^x \frac{dx}{W(x,t)}\right] \\ &\quad + \frac{\rho_g Q(t) S(t)}{\pi\rho}\int_0^x \frac{dx}{W(x,t)} \\ &\quad - \frac{\rho_g Q^2(t)}{2\rho\pi^2}\left[W^{-2}(0,t) - W^{-2}(x,t)\right]. \end{aligned} \tag{17}$$

Even limited by the leading term of order $\varepsilon^2\ln\varepsilon$, (17) remains integral-differential and the principle of independence is no more valid for unsteady ventilated cavities. In the case of a large velocity of the ventilated gas ($V = V'/U_\infty' \gg 1$) the last term in (17) is proportional to V^2 and is much greater than two previous terms proportional to V (see (12)). Thus, the shape of such slender intensively ventilated cavities can be estimated with the use of the following equation:

$$\begin{aligned} \varepsilon^2\ln\varepsilon Z(A) + O\left(\varepsilon^2\right) &= 0.5\sigma_0(t) \pm x\mathrm{Fr}^{-2}(t) \\ &\quad - \frac{\rho_g Q^2(t)}{2\rho\pi^2}\left[W^{-2}(0,t) - W^{-2}(x,t)\right] \end{aligned} \tag{18}$$

which does not contain any integral terms and corresponds to the Logvinovich independence principle.

To solve both (17) and (18), the standard initial and boundary conditions in two domains can be used (Nesteruk [28]):

$$\begin{aligned} x \ge \int_0^t \frac{dt}{\tau}: &\quad R(x,0) = R_1(x), \quad \frac{\partial R(x,0)}{\partial t} = R_2(x); \\ x \le \int_0^t \frac{dt}{\tau}: &\quad R(0,t) = R_3(t), \quad \frac{\partial R(0,t)}{\partial x} = R_4(t), \end{aligned} \tag{19}$$

where R_1, R_2, R_3, and R_4 are given functions.

5. Steady Ventilated Supercavities

In steady case (17) limited by the leading term of order $\varepsilon^2\ln\varepsilon$ attains the following form:

$$\frac{d^2R^2}{dx^2} = \frac{\sigma_0}{\ln\varepsilon} \pm \frac{2x}{\mathrm{Fr}^2\ln\varepsilon} + \Delta\left[a - \frac{1}{\left(R^2 - R_b^2\right)^2}\right], \tag{20}$$

$$\begin{aligned} \Delta &= -\frac{\rho_g Q^2}{\pi^2 R_0^4 \rho U_\infty^2 \ln\varepsilon}, \\ a &= \left[1 - \frac{R_{b0}^2}{R_0^2}\right]^{-2}, \end{aligned} \tag{21}$$

where all lengths are based on the cavity radius R_0 at its origin $x = 0$ (see Figure 1). Relation (20) follows also from (18), but in the steady case (20) is valid at arbitrary values of ventilation rate. To characterize the influence of gas injection, other nondimensional parameters can be used instead of Δ; for example,

$$Ve = -a\Delta\ln\varepsilon = \frac{\left(\rho_g V_0^2\right)}{\left(\rho U_\infty^2\right)} \quad \text{or } C_Q = \frac{Q}{\left(U_\infty \pi R_0^2\right)}, \tag{22}$$

where V_0 is the velocity of gas at $x = 0$. The dimensionless ventilation rate Ve is the ratio of the pressure heads in the gas and water flows at $x = 0$. If the gravity forces can be neglected also in liquid flow ($\mathrm{Fr} \to \infty$), nonlinear differential equation (20) coincides with the one obtained in Manova et al. [15].

With the use of parameter Ve (20) can be rewritten as follows:

$$\frac{d^2R^2}{dx^2} = \frac{\sigma_{\text{eff}}}{\ln\varepsilon} \pm \frac{2x}{\mathrm{Fr}^2\ln\varepsilon} - \frac{\Delta}{W^2}, \tag{23}$$

$$\sigma_{\text{eff}} = \sigma_0 - Ve = \sigma_0 - \frac{\left(\rho_g V_0^2\right)}{\left(\rho U_\infty^2\right)}, \tag{24}$$

$$W(x) = R^2(x) - R_b^2(x). \tag{25}$$

The standard initial conditions at $x = 0$

$$R = 1, \quad \frac{dR}{dx} = \beta \tag{26}$$

can be used to integrate (20) or (24), where β is the derivative of the body radius at the cavity origin. It can be seen from (20)

and (22) that the ventilation can strongly change the shape of the supercavity only at small values of $\sigma_0 \pm 2x/\mathrm{Fr}^2$ or at the large ratio V_0/U_∞, since ρ_g/ρ is very small.

Without ventilation ($\Delta = Ve = C_Q = 0$) equation (20) or (23) coincides with the one proposed in Nesteruk [32]. Its solution in this case can be easily obtained with the use of initial conditions (26):

$$R^2(x) = \frac{\sigma_0 x^2}{2\ln\varepsilon} \pm \frac{x^3}{3\mathrm{Fr}^2\ln\varepsilon} + 2\beta x + 1. \quad (27)$$

For ventilated supercavities the nonlinear differential equation (20) or (23) must be solved. It can be seen that gas injection strongly changes the cavity shape not only at great values of the parameter Δ but also at very small values of the circular channel width $R - R_b$.

The term in brackets in (20)

$$s_2(x) = W^{-2}(0) - W^{-2}(x) \quad (28)$$

equals zero at $x = 0$ and can be both positive and negative at different cavitator and hull shapes. It means that the corresponding ventilated cavity can, respectively, be both larger and smaller than the vapor one (27). Examples of calculations can be found in Manova et al. [15] and Nesteruk and Shepetyuk [16] for the first case and in Nesteruk and Shepetyuk [17] for the second one.

When the gravity forces can be neglected, (20) or (23) demonstrates that two independent parameters which are the pressure inside the cavity (σ_0) and the gas injection rate (Δ or Ve or C_Q) influence the cavity shape. The gas leakage from the stable artificial cavity is equal to the gas injection rate and depends on the cavity dimensions, cavity closing behaviour, and so forth. Therefore, the gas leakage can also be different at the fixed cavitation number (as the equal value of the gas injection rate). In particular, it is written in Logvinovich [1] that "it is impossible to suggest a universal method for the theoretical determination of the gas loss." This conclusion was supported by experiments (see, e.g., Wosnik et al. [10] and Vlasenko and Savchenko [13]), where different gas leakage/injection rates were obtained at the fixed cavitation number. Nevertheless, there are some attempts to present the gas leakage from the empty cavity ($R_b(x) \equiv 0$) at high Froude numbers as a function of cavitation number (see, e.g., Logvinovich [1] and Spurk [9]). At small Froude numbers in horizontal flow (the cavity has no more the axis of symmetry) the formulas representing the gas leakage rate as function of the cavitation and Froude numbers were proposed in Epshtein [2–4].

6. Different Cavitator Shapes and Restrictions of the Flow Parameters

The developed theory and equations can be applied for a different slender cavitator—a part of a hull wetted by water ($x < 0$). For example, the slope of the cavitator radius at the cavity origin section $x = 0$ can be both positive ($\beta > 0$; see Figure 1, a slender conical cavitator) and nonpositive ($\beta \le 0$; see Figure 2, a case of base cavities). In many applications the

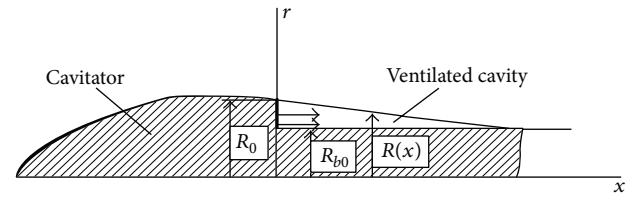

Figure 2: Base steady ventilated cavity ($\beta < 0$) on a cylindrical hull $R_b(x) = R_{b0} = \mathrm{const}$.

disc or nonslender conical cavitators are used to create a long supercavity. Equations (17), (20), and (23) can be used in the case of the nonslender cavitator too, provided that the initial part of the long cavity is known. In particular, in the steady case the Logvinovich empirical formula (Logvinovich [1])

$$R(x) = (1 + 3x)^{1/3}, \quad x < 3 \quad (29)$$

is valid. In (29) all lengths are based on the radius of the disc cavitator. In particular, from (29) it follows that at $x = x_s = 2$ the corresponding cavity radius and its slope are $R_s \approx 1.913$ and $\beta_s \approx 0.273$, respectively. If at $x > x_s$ the cavity is slender enough, we can use (20) with all lengths based on R_s. In the initial condition (26) β must be replaced by β_s. It is difficult to expect a good accuracy from such calculations, but an estimation of the supercavity shape is possible. In particular, at $\beta = \varepsilon$, $\mathrm{Fr} \to \infty$ the vapor cavity maximum radius can be determined from formula (27) as follows:

$$R_m = R_s\sqrt{1 - \frac{2\beta_s^2\ln\beta_s}{\sigma_0}} \approx 1.91\sqrt{\frac{\sigma_0 + 0.193}{\sigma_0}}. \quad (30)$$

Calculations of the maximum radius of the supercavity created by the disc cavitator with the use of the Logvinovich empirical formula (Logvinovich [1])

$$R_m \approx \sqrt{0.84\frac{\sigma_0 + 1}{\sigma_0}} \quad (31)$$

differ from (30) less than 10% at $0.001 < \sigma_0 < 0.1$.

It is important to know which values of parameters σ_0, Fr, and Ve are possible in real flows. To demonstrate the influence of the cavitator shape let us consider a vapor cavity in a liquid without gravity. The dependences (27) corresponding to $\beta > 0$ are presented in Figure 3 and attached to the case $\beta < 0$ in Figure 4. According to the stability principle, a small change in the parameters determining a solution ought to give rise to small changes in this solution.

At first let us consider the case $\beta > 0$. Since the parameter $\alpha = 0.5\sigma_0/\ln\varepsilon$ is negative at the positive cavitation numbers, then the branches of parabola (27) are directed to the bottom; accordingly at $\sigma_0 < 0$ they are directed upward. For zero cavity number the parabola (27) degenerates into linear dependence (see Figure 3). Such character of solution testifies about its steadiness at $\sigma_0 < 0$. But already at zero cavitation number the stability disappears, because at $\sigma_0 = 0$ formula (27) gives an infinite cavity, and at any positive

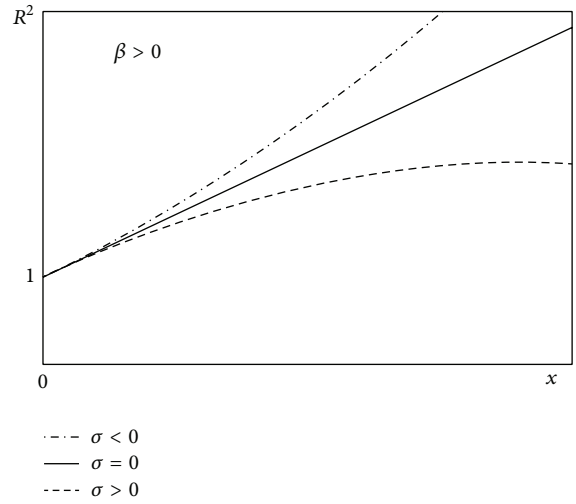

Figure 3: Dependences (27) for different values of the cavitation number at $\beta > 0$, Fr $\to \infty$.

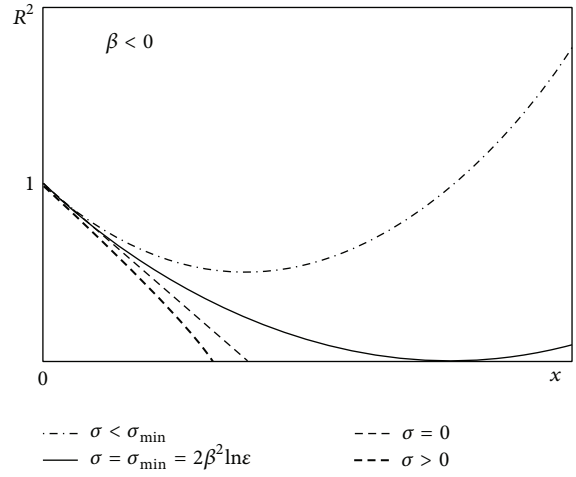

Figure 4: Dependences (27) for different values of the cavitation number at $\beta < 0$, Fr $\to \infty$.

cavitation number (which can be very near to zero) the cavity dimensions are bounded. The same character of instability takes place for $\beta = 0$. So, according to the stability principle only the flows with the positive cavitation numbers can be realized for cavitators with $\beta \geq 0$. The solution at $\sigma_0 = 0$ for such cavitators is unstable and has the theoretical meaning only.

For $\beta < 0$ the direction of parabola (27) branches does not change and it similarly degenerates into the linear dependence at zero cavitation number (see Figure 4). But due to the negative value of parameter β, the zero cavitation number corresponds to a bounded cavity. The bounded cavities exist also for some negative cavitation numbers (small enough for module (see Figure 4)). Critical value of $\sigma_0 = \sigma_{\min} < 0$ corresponds to the case when the parabola (27) touches the axis x. At cavitation numbers, lesser than $\sigma_{\min}$, cavity is unbounded. Application of the stability principle yields that at $\beta < 0$ only flows with $\sigma_0 < \sigma_{\min} < 0$ can be realized. At $\beta < 0$, Fr $\to \infty$ the minimum cavitation number may be defined from (27) as follows: $\sigma_{\min} = 2\beta^2 \ln \varepsilon$ (Nesteruk [32]).

In the case of liquid with gravity the limitations of values of parameters σ_0, Fr follow from (27). Specifically, for the steady flow directed to the bottom, the coefficient $1/(3\mathrm{Fr}^2 \ln \varepsilon)$ of the polynomial (27) is negative; therefore a cavity always has the bounded dimensions, and steadiness principle is valid for arbitrary values of σ_0, Fr. For the opposite direction of the flow, this coefficient changes its sign, and the situation is similar to the case shown in Figure 4. The dependences of the minimum cavitation number versus the Froude number are calculated in Nesteruk [32].

The stability principle can be used to analyze the parameter restrictions for unsteady supercavity flows too. An example of a slender axisymmetric cavitator located in the steady flow of liquid with gravity directed upwards with the cavitation number, which varies according to the linear law $\sigma_0(t) = \sigma_0(0) - a_0 t$, is presented in Nesteruk [35]. In this flow the pressure inside the cavity is only time dependent and we can use (6) with $C_p(x,t) = -\sigma_0(t) = -\sigma_0(0) + a_0 t$ or (17) with $Q(t) = 0$. The solution of the equation of the first approximation (9) in this case can be written as follows (see Nesteruk [35]):

$$R^2(x,t) = \frac{\sigma(t)\, x^2}{2\ln\varepsilon} + \frac{x^3\left(a_0 - \mathrm{Fr}^{-2}\right)}{3\ln\varepsilon} + 2R_0\beta x + R_0^2. \quad (32)$$

If the parameter a_0 satisfies the condition $0 < a_0 < \mathrm{Fr}^{-2}$, then a moment of time t_c comes, when the cavity becomes unbounded for $t > t_c$. The critical cavitation number $\sigma_c = \sigma_0(t_c)$ can be also calculated. For example, for $\beta = 0$ the formula $\sigma_c = \left[-6(\mathrm{Fr}^{-2} - a_0)^2 \ln \varepsilon\right]^{1/3}$ can be obtained from (32). Thus, the diminishing of the cavitation number to the value lesser than critical is impossible. Probably, the supercavity flow pattern is lost in the moment when $\sigma = \sigma_c$.

It is interesting to emphasize that such flow of a liquid without gravity is always stable. Really, it follows from (32) that, when the cavitation number diminishes ($a_0 > 0$), the cavity dimensions are finite both at the negative and at positive current values of the cavitation number $\sigma_0(t)$. According to (32) the cavity dimensions diminish continuously when the cavitation number increases. In particular, there are possible unsteady supercavity flows with a conical cavitator at negative cavity numbers, while steady flows are impossible at $\sigma_0 < 0$.

In this example we considered the evolutions of the cavity shape forced by the changes of the pressure inside the cavity only (or by the variations of the cavitation number σ_0). Solution (32) is independent of the shape of the hull located inside the cavity. At small values of the area of the circular channel between the cavity surface and the hull ($W(x,t) \ll 1$) equation (17) must be used. In particular, we show in the next sections that for the flows with ventilated supercavities their parameters restrictions depend on the pressure, ventilation rate, and the shape of the hull located inside the cavity.

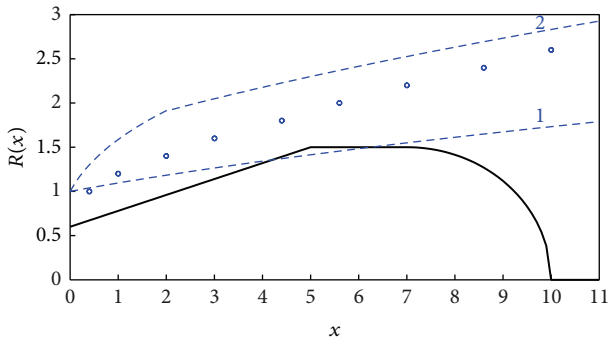

FIGURE 5: Hull shape (35) ($R_{b0} = 0.6$; $R_{b1} = 1.5$; $x_1 = 5$; $x_2 = 7$; $x_3 = 10$; solid line) and critical infinite cavity shapes at zero cavitation number and Fr $\to \infty$ for two different cavitators (dashed line 1 corresponds to (37) at $\beta = 0.1$; dashed line 2 corresponds to the disc cavitator (38)).

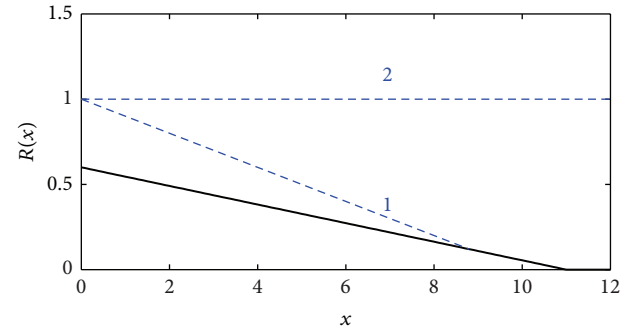

FIGURE 6: Hull shape (36) ($R_{b0} = 0.6$; $x_1 = 11$; solid line) and critical base cavity shapes at minimal cavitation numbers and Fr $\to \infty$ for two different cavitators (dashed line 1 corresponds to $\sigma_{\min} = 2\beta^2 \ln \varepsilon$ (39) at $\beta = -0.1$; dashed line 2 corresponds to (37) at $\beta = 0$).

7. Cavities on Different Hulls

Let us assume the shape of the hull located in the cavity to be a combination of functions as follows:

$$R_b(x) = \sqrt{\alpha_i (x - x_i)^2 + 2\beta_i (x - x_i) + R_{bi}^2}, \quad x_i \le x \le x_{i+1}; \quad i = 0, 1, 2, \ldots, k-1; \quad x_0 = 0, \tag{33}$$

$$R_b(x) = R_{bk}; \quad x > x_k. \tag{34}$$

Constants R_{bi} coincide with the values of the hull radius at $x = x_i i = 0, 1, 2, \ldots, k$; that is, $R(x_i) = R_{bi}$. Constants β_i and α_i can be chosen to ensure the continuity of the hull radius and its slope at $x = x_i$; $i = 1, 2, \ldots, k-1$. The hull shapes can be finite ($R_{bk} = 0$) and infinite ($R_{bk} > 0$). Examples of such shapes are presented by the following formulas and shown in Figures 5 and 6 by solid lines:

$$R_b(x) = \begin{cases} R_{b0} + \dfrac{x(R_{b1} - R_{b0})}{x_1}, & 0 \le x \le x_1 \\ R_{b1}, & x_1 \le x \le x_2 \\ \sqrt{R_{b1}^2 - \dfrac{(x - x_2)^2 R_{b1}^2}{(x_3 - x_2)^2}}, & x_2 \le x \le x_3 \\ 0, & x \ge x_3, \end{cases} \tag{35}$$

$$R_b(x) = \begin{cases} R_{b0} - \dfrac{x R_{b0}}{x_1}, & 0 \le x \le x_1 \\ 0, & x \ge x_1. \end{cases} \tag{36}$$

By increasing the number of k, arbitrary time independent hull shape can be interpolated by formulas (33) with a rather good accuracy. We will use these formulas in the next section to obtain a steady problem solution. Here we will try to answer the very important question: is it possible to cover any given hull by one steady cavity with the origin at the cross section $x = 0$?

Let us consider the critical cavity shapes corresponding to the minimal possible values of the cavitation number $\sigma_0 = \sigma_{\min}(\mathrm{Fr})$. In particular, in the flow without gravity (Fr $\to \infty$) the minimal possible cavitation number is zero at $\beta \ge 0$ and the corresponding critical cavity shape can be determined from (27) as follows:

$$R(x) = \sqrt{2\beta x + 1}. \tag{37}$$

In the case of the disc cavitator the critical cavity shape can be estimated with the use of (29) and (27) and continuity condition at $x_s = 2$:

$$R(x) \approx \begin{cases} (1 + 3x)^{1/3}, & 0 \le x \le 2 \\ \sqrt{0.546(x - 2) + 1.913^2}, & x \ge 2. \end{cases} \tag{38}$$

Examples of the critical cavity shape (37) are presented in Figure 5 by dashed line 1 ($\beta = 0.1$) and in Figure 6 by dashed line 2 ($\beta = 0$). An example of the critical cavity shape (38) for the disc cavitator is presented in Figure 5 by dashed line 2.

For the base cavities at $\beta < 0$, Fr $\to \infty$ the minimal possible cavitation number is $\sigma_{\min} = 2\beta^2 \ln \varepsilon$ and the corresponding conical critical cavity shape can be determined from (27) as follows:

$$R(x) = \beta x + 1. \tag{39}$$

An example of the critical cavity shape (39) is presented in Figure 6 by dashed line 1 ($\beta = -0.1$).

If the hull pierces the corresponding critical cavity shape (e.g., dashed lines 1 in Figures 5 and 6), then it is impossible to cover such hull with one cavity starting at the cross section $x = 0$. Neither the cavity pressure increase (diminishing the cavitation number σ_0) nor increasing the gas injection rate can create a cavity covering all the hull. It is possible only to cover the part of the hull located upstream to the piercing region (e.g., at $x \le x_1$ for case $\beta = 0.1$ shown in Figure 5) or to use other cavities, for example, the ones starting at the cross sections $x = x_1$ and $x = x_2$ on the hull shown in Figure 5.

For the vapor cavities on conical-cylindrical hulls ($x_2 \to \infty$ in (30)), a similar limitation was revealed in Nesteruk [36]. It was shown that a cavity created by a slender cone can close on the cylindrical part only if $R_{01} < \sqrt{2\beta x_1 + 1}$

(in accordance with (37)). If the radius of the cylindrical part is greater than value $\sqrt{2\beta x_1 + 1}$, all the cavities close on the conical part. For such cavities both the positive and the negative cavitation numbers are possible (the stability occurs in all these cases) and their shapes can be both convex and concave (Nesteruk [36]).

If the hull (35) touches the critical cavity shape only in one cross section $x = x_1$, then the maximum length of the cavity closing on the conical part (or the minimal length of the cavity $L_{\min}$ closing on the cylindrical part) is equal to x_1 (the cavity length is calculated along the axis of symmetry). Then the relationship between $x_1 = L_{\min}$ and the radius of the conical part R_{b1} coincides with (37) or (38) after replacing x_1 instead of x and R_{b1} instead of $R(x)$. In Varghese et al. [37] the cavities created by the disk cavitator were calculated with the use of nonlinear approach and the dependence of the minimum cavity length $L_{\min}$ versus the cylindrical part radius R_{b1} was revealed (no convergence was achieved at the values of cavity length smaller than $L_{\min}$). The numerical results from the paper (Varghese et al. [37]) are shown in Figure 5 by markers. The rather good agreement between the data of Varghese et al. [37] and dashed line 2 supports the conclusions of the presented analysis and illustrates the accuracy of the Logvinovich formula (29) and the first approximation (27).

Any hull of bounded dimensions located under the corresponding critical cavity shape (like dashed lines 2 in Figures 5 and 6) can be entirely covered by a supercavity at zero gas injection rate Ve by increasing the pressure inside the cavity or by reducing the cavitation number σ_0. If the cavitation number σ_0 is not small enough, the corresponding supercavity closes on the hull.

In many cases the ventilation increases the supercavity dimensions at fixed σ_0 (see Section 5, Manova et al. [15], and Nesteruk and Shepetyuk [16]). If the increase of the pressure at $x = 0$ (or diminishing σ_0) is impossible we could try to cover the hull by the cavity entirely only by increasing the gas injection rate. Equations (23) and (24) and a numerical solution of (23) obtained in Nesteruk and Shepetyuk [16] show that it is possible only for small enough values of σ_0. The ventilation decreases the effective cavity number (see (24)) and corresponding cavity must be larger (see (27) at $\sigma_0 = \sigma_{\text{eff}}$). On the other hand, according to the last term in (23) the ventilated cavity is smaller than the vapor one at $\sigma_0 = \sigma_{\text{eff}}$. Thus, covering the hull by the cavity at small values of the gas pressure depends on the values of the ventilation rate and σ_0.

Let us illustrate this conclusion by an example of the numerical solution of (23) obtained in Nesteruk and Shepetyuk [16] for conical-cylindrical hulls ($x_2 \to \infty$ in (30), $\beta = \varepsilon = 0.1$, $R_{b0} = 0.8$, and Fr $\to \infty$; see Figure 7). The values of $x_1 = 17$ and $R_{b1} = 2$ correspond to the hull located under the corresponding critical cavity shape $R_{01} < \sqrt{2\beta x_1 + 1}$ (in accordance with (37)). At the small fixed cavitation number $\sigma_0 = 0.01$ it is possible to have a cavity which closes on the cylindrical part. In this case the cavity length L_c can be rather good estimated with the use of linear theory—(27) at $\sigma_0 = \sigma_{\text{eff}}$. In particular, the discontinuity of L_c takes place (similar to the one revealed in Varghese et al. [37] and Nesteruk [36] for vapor cavities). If $\sigma_{\text{eff}} \to 0$ (or

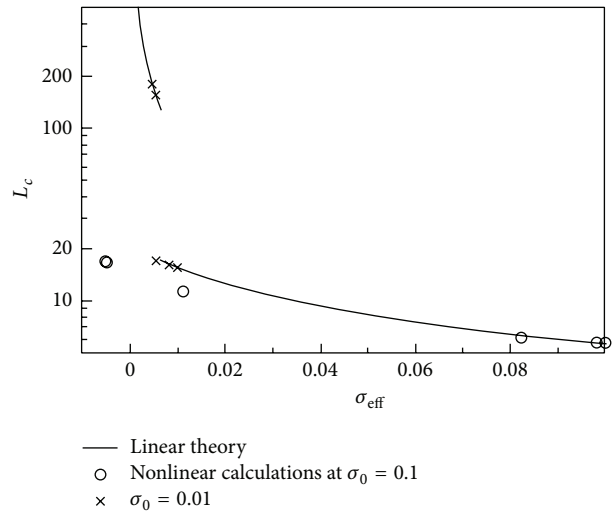

Figure 7: The length of ventilated cavities on conic-cylindrical bodies at $x_1 = 17$, $R_{b1} = 2$, $R_{b0} = 0.8$, $\beta = \varepsilon = 0.1$, and Fr $\to \infty$ (Nesteruk and Shepetyuk [16]).

$Ve \to \sigma_0$) the cavity becomes unbounded. It means that ventilation rate is limited by the value

$$\Delta^{\text{cr}} = -\frac{\sigma_0}{a \ln \varepsilon} \quad \text{or } Ve^{\text{cr}} = \sigma_0. \tag{40}$$

At $\sigma_0 = 0.1$ the cavity closes only on conical part of the hull ($L_c \le x_1$) and there is a large difference between the linear theory and nonlinear calculations based on (23). The gas injection rate is limited by some other critical value ($\Delta^{\text{cr}} \approx 0.00593$ or $Ve^{\text{cr}} \approx 0.105$). Formally, a solution exists at greater values of ventilation, but the cavity becomes infinite at $\Delta \approx 0.00593$ and such flow cannot be real.

Thus, covering the hulls located under the corresponding critical cavity shapes by ventilated cavities must be investigated with the use of solutions of nonlinear equation (20) or (23). In the next section it will be shown that in the case Fr $\to \infty$ the resolving (20) can be reduced to the calculation of simple integrals.

8. Solution of the Steady Problem at High Froude Numbers

8.1. Integral Formula for the Solution. The nonlinear differential equation (20) or (23) can be solved numerically at any value of the Froude number and for any shape of the hull located inside the cavity. Let us consider the case Fr $\to \infty$ and the hulls which can be presented or interpolated as (33). Substituting $R^2(x) = W(x) + R_b^2(x)$ into (23) and using (33) yield

$$\frac{d^2W}{dx^2} = \frac{\sigma_{\text{eff}}}{\ln \varepsilon} - 2\alpha_i - \frac{\Delta}{W^2}, \qquad x_i < x < x_{i+1}; \quad i = 0, 1, 2, \ldots, k-1; \ \alpha_k = 0, \ x > x_k. \tag{41}$$

The initial conditions (26) at $x = 0$ can be rewritten as follows:

$$W = 1 - R_{b0}^2, \qquad \frac{dW}{dx} = 2\beta - 2\beta_0. \tag{42}$$

Let us assume the function $W(x)$ to be continuous at points $x = x_i$; $i = 1, 2, \ldots, k$. Its derivative dW/dx can be discontinuous at these points if the slope of the hull contour is discontinuous (e.g., at $x = x_1$ for the hull shape shown in Figure 5). It means that, for every segment $x_i < x < x_{i+1}$, $i = 0, 1, 2, \ldots, k-1$, and the segment $x > x_k$, the specific initial conditions should be used at the beginning of each segment $x = x_i$, $i = 0, 1, 2, \ldots, k$:

$$W = R^2(x_i) - R_{bi}^2 = W_i,$$
$$\frac{dW}{dx} = \left.\frac{dR^2}{dx}\right|_{x=x_i} - 2\beta_i = u_i. \tag{43}$$

The order of (41) can be reduced by substitutions $dW/dx = u$ and $d^2W/dx^2 = du/dx = udu/dW$. With the use of initial conditions (43) the following first-order equation can be obtained:

$$u^2 = 2\left(\frac{\sigma_{\text{eff}}}{\ln\varepsilon} - 2\alpha_i\right)(W - W_i) + 2\Delta\left[\frac{1}{W} - \frac{1}{W_i}\right] + u_i^2, \qquad x_i < x < x_{i+1}. \tag{44}$$

Equation (44) can be integrated with the use of initial conditions (43):

$$x - x_i = \pm\int_{W_i}^{W} \frac{\sqrt{\xi}\,d\xi}{\sqrt{a_i\xi^2 + b_i\xi + 2\Delta}}, \qquad x_i \le x \le x_{i+1}, \tag{45}$$

$$a_i = 2\left(\frac{\sigma_{\text{eff}}}{\ln\varepsilon} - 2\alpha_i\right);$$
$$b_i = u_i^2 - 2W_i\left(\frac{\sigma_{\text{eff}}}{\ln\varepsilon} - 2\alpha_i\right) - \frac{2\Delta}{W_i}. \tag{46}$$

Sign "+" or "−" must be used in (45) according to the value of $u = dW/dx$.

The cavity closing corresponds to the zero value of $W(x)$, but from the physical point of view it is impossible to have the zero cross section area of gas flow in the steady ventilated cavity and from the mathematical point of view it is impossible to achieve the zero value of $W(x)$, since the differential equation (41) has a discontinuity. To avoid these difficulties we will suppose that the cavity "closure" corresponds to some small positive value of W (e.g., $W = 0.0001$). Then the cavity length (along the axis of symmetry) can be also calculated from integral relations (45).

8.2. Maximum and Minimum Values of the Circular Channel Area. The inverse function $x = x(W)$ may be many-valued (see curves 4 and 5 in Figure 8). In this case it is necessary to integrate in (45) from W_i to W_{ex} corresponding to the maximum or the minimum value of the gas flow cross section area in the circular channel between the cavity surface and the hull and then to integrate from W_{ex} to W with the opposite sign in (45). The values of W_{ex} can be easily calculated from the quadratic equation following from (44) at $u = 0$:

$$a_iW_{ex}^2 + b_iW_{ex} + 2\Delta = 0. \tag{47}$$

If $a_i \neq 0$, the maximum value of W can be calculated from (47) as follows:

$$W_{\max} = \frac{-b_i - \sqrt{b_i^2 - 8\Delta a_i}}{2a_i}. \tag{48}$$

An example of the cavity with the maximum value of W (for $a_i < 0$, $b_i > 0$) is presented in Figure 8 (curve 4). At $a_i \ge 0$ the maximum of W exists only for $b_i < 0$. In particular, at $a_i = 0$ it follows from (22), (24), (46), and (47) that

$$W_{\max} = -\frac{2\Delta}{b_i}, \qquad \sigma_0 > \ln\varepsilon\left(2\alpha_i - \frac{u_i^2}{2W_i}\right). \tag{49}$$

The minimum of W exists only for $a_i > 0$ and $b_i < 0$ and can be calculated from (47) as follows:

$$W_{\min} = \frac{-b_i + \sqrt{b_i^2 - 8\Delta a_i}}{2a_i}. \tag{50}$$

An example of the cavity with the minimum value of W is presented in Figure 8 (curve 6).

It must be noted that among the cavities presented in Figure 8 only curves 4 and 9 have classical elliptical shapes. Cavities 3 and 8 are parabolic, 2 and 7 are conical, 1 and 6 are hyperbolic, and 5 is cylindrical. If $x_1 \to \infty$, it is possible to realize only cavities 4, 7, 8, and 9. Other cavities cannot exist in reality without conical part of the hull ($x_1 \le x \le x_2$) according to the stability principle mentioned above.

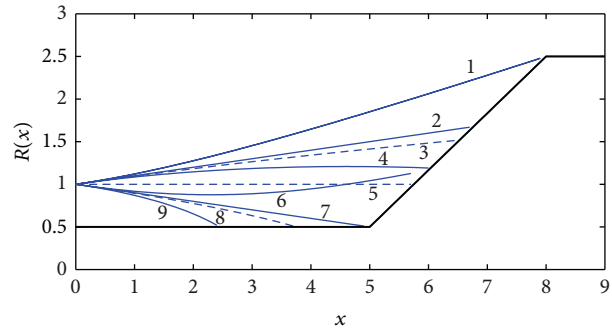

FIGURE 8: The cavity shapes (27) at zero ventilation rate on a conic-cylindrical hull ($x_1 = 5$, $x_2 = 8$, $R_{b0} = R_{b1} = 0.5$, $R_{b2} = 2.5$, $\varepsilon = 0.1$, and Fr $\to \infty$) for $\beta = 0.1$ (curves 1–4, the corresponding values of σ_0 are −0.2626, −0.046, 0, and 0.1, resp.), for $\beta = 0$, $\sigma_0 = 0$ (curve 5), and for $\beta = -0.1$ (curves 6–9, the corresponding values of σ_0 are −0.2, −0.046, 0, and 0.2, resp.). The cavity shapes corresponding to the zero cavitation number (curves 3, 5, and 8) are shown by dashed lines.

The cavity shapes corresponding to the zero cavitation number (dashed curves 3, 5, and 8) do not cover the hull shown in Figure 8. It means that at any value σ_0 and at any ventilation rate all 3 cavitators (with $\beta = 0.1$, 0, and -0.1) cannot create a cavity large enough to cover the hull.

8.3. Degenerate Solutions, Neutral Hull Shapes, and Critical Values of the Ventilation Rate. Equation (41) can be rewritten as follows (with the use of (22), (24), and (43)):

$$\frac{d^2W}{dx^2} = \frac{\sigma_i}{\ln\varepsilon} - 2\alpha_i + \Delta\left(\frac{1}{W_i^2} - \frac{1}{W^2}\right),$$
$$\sigma_i = \sigma_0 + \Delta\ln\varepsilon\left(\frac{1}{W_0^2} - \frac{1}{W_i^2}\right); \quad (51)$$
$$x_i < x < x_{i+1}; \quad i = 0, 1, 2, \ldots, k-1.$$

If

$$\frac{\sigma_i}{\ln\varepsilon} - 2\alpha_i = 0; \qquad u_i = 0, \quad (52)$$

then (51) has the obvious solution $W(x) \equiv W_i = \text{const}$ at any value of the ventilation rate. The inverse function $x = x(W)$ is many-valued and such degenerate solution cannot be obtained with the use of (45). Relationship (33) in view of (43) and (52) allows calculating the corresponding body shape

$$R_b(x) = \sqrt{\frac{0.5\sigma_i x^2}{\ln\varepsilon} + 2\beta_i x + R_{bi}^2}, \quad (53)$$
$$x_i < x < x_{i+1}; \; i = 0, 1, 2, \ldots, k-1.$$

For example, for the part of the hull, corresponding to $0 \le x \le x_1$ and shown in Figure 8, $R_b(x) \equiv R_{b0}$. Therefore (53) yields $\beta = 0$ and $\sigma_0 = 0$. The degenerate solution $R(x) \equiv 1$ is shown in Figure 8 by straight line 5. The hull (53) ensures the same cavity shape at any ventilation rate. This shape coincides with the shape of the vapor cavity at the same values of parameters σ_0 and β and can be refereed as neutral.

Equation (20) demonstrates that for $W(x) > W_0$ the ventilation increases the cavity dimensions. For example, at $0 \le x \le x_1$ the dimensions of cavities 1–4 shown in Figure 8 for $\Delta = 0$ will increase with increasing the ventilation rate. The maximum cavity radius can be also infinite, if the cavity covers all the hull or the hull is unbounded (e.g., $x_1 \to \infty$). Formulas (46) and (48) allow calculating the critical ventilation rate corresponding to zero value of a_i

$$Ve_1^{(\mathrm{cr})} = \sigma_0 - 2\alpha_i\ln\varepsilon$$
$$\text{or } \Delta_1^{(\mathrm{cr})} = \frac{\left(2\alpha_i\ln\varepsilon - \sigma_0\right)}{(a\ln\varepsilon)}. \quad (54)$$

If inequality (49) is valid, the cavity is bounded at the ventilation rates (54) but for $a_i > 0$ the value of $b_i^2 - 8\Delta a_i$ in (48) can be zero or negative. The equation $b_i^2 - 8\Delta_2^{(\mathrm{cr})}a_i = 0$ yields the second critical value, which with the use of (46) can be represented as follows:

$$\Delta_2^{(\mathrm{cr})} = \frac{W_i\left(u_i^2 - 2W_i\left(\sigma_0/\ln\varepsilon\right)\right)^2}{8u_i^2}. \quad (55)$$

If $\Delta \le \Delta_2^{(\mathrm{cr})}$, the corresponding cavity is bounded, but unbounded at $\Delta > \Delta_2^{(\mathrm{cr})}$. It means that the ventilation rate is limited by the value $\Delta_2^{(\mathrm{cr})}$. For unbounded cylindrical hulls the critical ventilation rates were calculated in Manova et al. [15] and coincide with (54) and (55).

On the other hand, for $W(x) < W_0$ the ventilation decreases the cavity dimensions. For example, the dimensions of cavities 6–9 shown in Figure 8 for $\Delta = 0$ will decrease with increasing the ventilation rate at $0 \le x \le x_1$. In particular, according to the formula (50) the $W_{\min}$ decreases from value $-b_i/a_i$ at $\Delta = 0$ to $-0.5b_i/a_i$ at $\Delta = b_i^2/(8a_i)$. The equation $b_i^2 - 8\Delta_2^{(\mathrm{cr})}a_i = 0$ yields the critical value, presented by (55). If $\Delta \le \Delta_2^{(\mathrm{cr})}$, the corresponding cavity has a minimum, but increasing the ventilation rate over the critical value diminishes the cavity dimensions and its shape has no minimum.

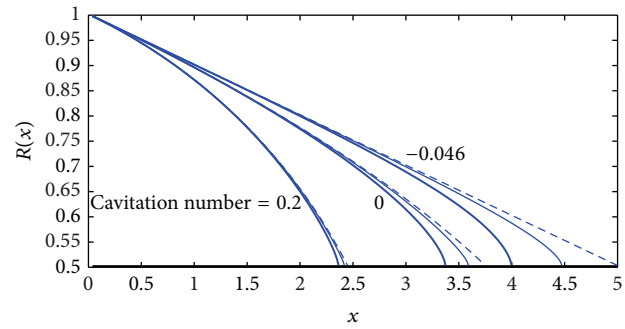

FIGURE 9: The cavity shapes on a conic-cylindrical hull ($\beta = -0.1$, $x_1 = 5$, $x_2 = 8$, $R_{b0} = R_{b1} = 0.5$, $R_{b2} = 2.5$, $\varepsilon = 0.1$, and $\mathrm{Fr} \to \infty$) for different values of the cavitation number ($\sigma_0 = -0.046$, 0, and 0.2) and different gas injection rates (dashed lines correspond to $\Delta = 0$, solid lines to $\Delta = 0.0005$, and solid bold lines to $\Delta = 0.002$).

8.4. Examples of the Ventilated Cavity Shape Calculations. If the pressure in the cavity at some cross section is fixed (e.g., the cavitation number σ_0 is fixed) and $u_i < 0$ (the area of the circular gas channel diminishes), the increase of the gas injection rate yields the diminishing of the cavity dimensions (since local pressure in the cavity diminishes). This fact is illustrated by the calculation examples shown in Figures 9 and 10. In both cases $u_0 = 2\beta - 0 = -0.2 < 0$ and the increasing of the gas injection rate decreases the cavity dimensions at $0 \le x \le x_1$. To calculate the cavities at $x > x_1$ the values W_1 and u_1 were used according to formulas (43). The values u_1 are also negative for all cavities shown in Figure 10.

Curve 4 shown in Figure 10 corresponds to the critical value of gas injection rate $\Delta = \Delta_2^{(\mathrm{cr})} \approx 0.0191$ calculated from (55). At greater values of Δ (curves 5–7) cavity shape has no minimum. At smaller and zero values of the gas injection

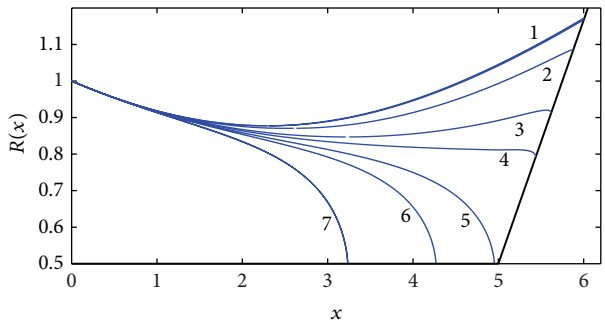

FIGURE 10: The cavity shapes on a conic-cylindrical hull ($\beta = -0.1$, $x_1 = 5$, $x_2 = 8$, $R_{b0} = R_{b1} = 0.5$, $R_{b2} = 2.5$, $\varepsilon = 0.1$, and Fr $\to \infty$) for the cavitation number $\sigma_0 = -0.2$ and different gas injection rates ($\Delta = 0$, 0.005, 0.015, 0.0191, 0.025, 0.03, and 0.05 for curves 1–7, resp.). Curve 4 corresponds to the critical value of gas injection rate $\Delta = \Delta_2^{(cr)}$ (see (55)).

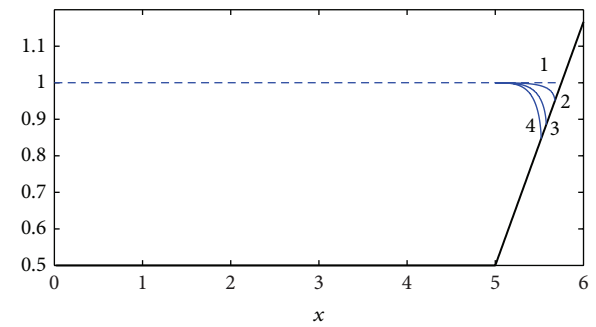

FIGURE 11: The cavity shapes on a conic-cylindrical hull ($\beta = 0$, $x_1 = 5$, $x_2 = 8$, $R_{b0} = R_{b1} = 0.5$, $R_{b2} = 2.5$, $\varepsilon = 0.1$, and Fr $\to \infty$) for the cavitation number $\sigma_0 = 0$ and different gas injection rates ($\Delta = 0$, 0.1, 0.5, and 1.0 for curves 1–4, resp.).

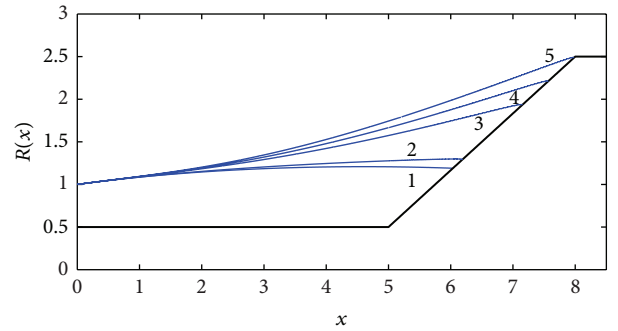

FIGURE 12: The cavity shapes on a conic-cylindrical hull ($\beta = 0.1, x_1 = 5$, $x_2 = 8$, $R_{b0} = R_{b1} = 0.5$, $R_{b2} = 2.5$, $\varepsilon = 0.1$, and Fr $\to \infty$) for the cavitation number $\sigma_0 = 0.1$ and different gas injection rates $\Delta = 0$, 0.02591, 0.1, 0.126, and 0.148 (curves 1–5, resp.).

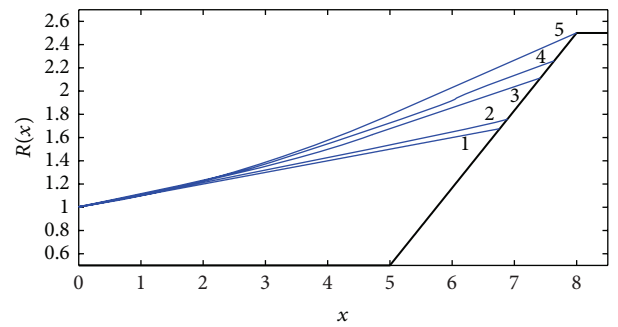

FIGURE 13: The cavity shapes on a conic-cylindrical hull ($\beta = 0.1$, $x_1 = 5$, $x_2 = 8$, $R_{b0} = R_{b1} = 0.5$, $R_{b2} = 2.5$, $\varepsilon = 0.1$, and Fr $\to \infty$) for the cavitation number $\sigma_0 = -0.046$ and different gas injection rates $\Delta = 0$, 0.01, 0.05, 0.064, and 0.087 (curves 1–5, resp.).

rate (curves 1–3) cavity shapes have a minimum point and some of them (curves 2 and 3) have also a maximum located near the closing on the conical part of the hull. For $\beta = 0$ and $\sigma_0 = 0$ the hull presented in Figure 8 corresponds to the neutral shape (53) at $0 \le x \le x_1$. It means that at $0 \le x \le x_1$ the corresponding cylindrical cavity shape (shown in Figure 8 by curve 5) is the same at any values of ventilation. Since the value u_1 is negative, at $x > x_1$, at this segment the cavity radius diminishes as the gas injection rate increases. The examples of calculations are shown in Figure 11.

Absolutely different behavior occurs in the case $u_i > 0$, when the area of the circular gas channel increases. The dimensions of the ventilated cavities increase as the gas injection rate increases. This fact is illustrated by the calculation examples shown in Figures 12 and 13. In both cases $u_0 = 2\beta - 0 = 0.2 > 0$. To calculate the cavities at $x > x_1$ the values W_1 and u_1 were used according to formulas (43). At great enough values of the cavitation number σ_0, the cavity shapes transform from convex with the maximum thickness section at small values of the gas injection rates (see Figure 12, curves 1 and 2) to the concave at greater values of Δ. At $\sigma_0 \ge -0.046$ the cavity shapes are concave (see, e.g., Figure 13). All the cavities cannot be extended for $x > x_2 = 8$ (according to the stability principle); thus the values of gas injection rate are limited. For example, for the case shown in Figure 12 the critical value $\Delta^{(cr)} \approx 0.148$. At smaller values of σ_0 the critical values of the gas injection rate diminish (e.g., at $\sigma_0 = -0.046$ $\Delta^{(cr)} \approx 0.087$ (see Figure 13) and at $\sigma_0 = -0.2626$ $\Delta^{(cr)} \approx 0.00025$). It must be noted that for the hull shape shown in Figures 8–13 the cavities corresponding to the critical values (54) and (55) are bounded (since x_1 is restricted). For example, the cavity shape corresponding to the critical value of the ventilation $\Delta_2^{(cr)} \approx 0.02591$ is shown in Figure 12 by curve 2.

8.5. Cavity Closing Near the Hull Contour Discontinuities. A special attention should be paid to the cases when the cavity end passes through the hull contour discontinuity $L_c \approx x_i$ as shown in Figures 14 and 15. If $dR^2/dx|_{x=x_i} < 2\beta_i$ or $u_i < 0$ (see (43)), the cavity length varies continuously. This case is shown in Figure 14. Absolutely different is the case $u_i > 0$ shown in Figure 15. At some critical values of parameters Δ and σ_0 the cavity contour touches the hull at the point $x = x_i$, and a "jump" in the cavity length is possible (see Figure 15).

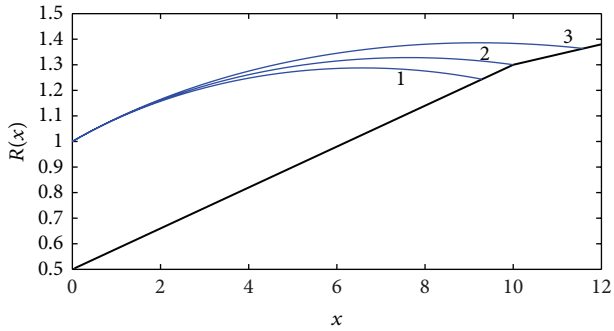

FIGURE 14: The cavities at $\Delta = 0$, Fr $\to \infty$, and $\beta = \varepsilon = 0.1$ on the conic-conic hull ($x_1 = 10$, $R_{b0} = 0.5$, $R_{b1} = 1.3$, and $\beta_1 = 0.052$) for cavitation numbers $\sigma_0 = 0.05$, 0.0603, and 0.07 (curves 1–3, resp.).

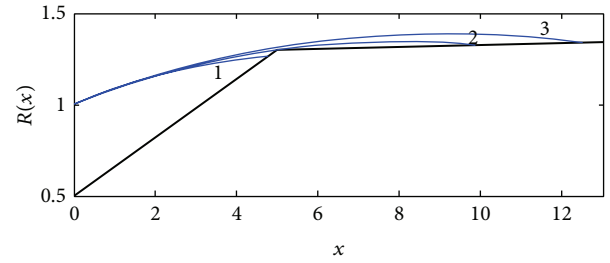

FIGURE 15: The cavities at $\Delta = 0$, Fr $\to \infty$, and $\beta = \varepsilon = 0.1$ on the conic-conic hull ($x_1 = 5$, $R_{b0} = 0.5$, $R_{b1} = 1.3$, and $\beta_1 = 0.0065$) for cavitation numbers $\sigma_0 = 0.05$, 0.057, and 0.07 (curves 1–3, resp.).

These two cases of cavity behaviour are separated by the condition $u_i = 0$ at $L_c = x_i$ or

$$\left.\frac{dR^2}{dx}\right|_{x=x_i} = 2\beta_i, \tag{56}$$

$$R^2\big|_{x=x_i} = R_{bi}^2. \tag{57}$$

At $\Delta = 0$ formulas (56) and (57) allow obtaining the relationships between the critical values of parameters x_i, β_i, and R_{bi}. With the use of (27), equation (56) can be written as follows:

$$\frac{\sigma_c x_i}{\ln \varepsilon} + 2\beta = 2\beta_i, \tag{58}$$

where the critical value of the cavitation number σ_c may be determined from (57) as follows:

$$\frac{\sigma_c x_i^2}{2 \ln \varepsilon} + 2\beta x_i + 1 = R_{bi}^2. \tag{59}$$

Finally, from (58) and (59) the following simple relationship can be obtained:

$$R_{bi}^2 = (\beta + \beta_i)\, x_i + 1. \tag{60}$$

In the particular case of a conic-cylindrical hull ($\beta_i = 0$), (60) coincides with the relationship proposed in Nesteruk [36]. When the value of R_{bi} is smaller than the critical one

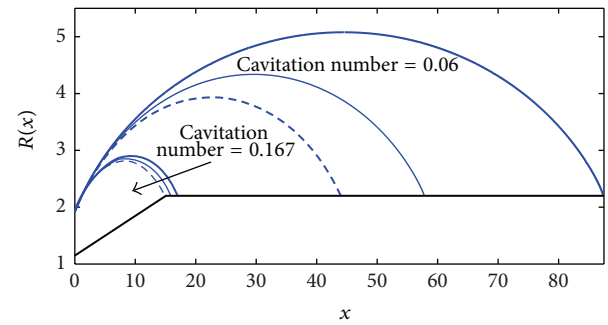

FIGURE 16: The cavities at Fr $\to \infty$ created by a disc cavitator located at $x = -2$ for the conic-cylindrical hull ($x_1 = 15$, $R_{b0} = 1.15$, and $R_{b1} = 2.2$) used in Vlasenko and Savchenko [13]. At $x < 0$ the cavity shape is represented by formula (29); at $x > 0$ the values $\beta = \varepsilon = \beta_s \approx 0.273$ are used in (45) for two cavitation numbers $\sigma_0 = 0.167$ and $\sigma_0 = 0.06$ and three values of gas injection rates $\Delta = 0$ (dashed lines), $\Delta = 0.005$ (solid lines), and $\Delta = 0.01$ (bold lines).

(60) and $L_c \approx x_i$, the cavity length varies continuously as shown in Figure 14. Otherwise the cavity length has a discontinuity as shown in Figure 15. For the ventilated cavities the critical values of parameters x_i, β_i, and R_{bi} depend on Δ and should be calculated with the use of (45). For the conic-cylindrical hull some examples can be found in Nesteruk and Shepetyuk [16] and are shown in Figure 7.

In the case $u_i < 0$ a rather weak dependence of the cavity length on the ventilation rate should be expected. Even in the case when cavity dimensions increase with increasing Δ at $x < x_i$, the negative value of u_i leads to a decrease of the cavity length at $x > x_i$. This fact is illustrated in Figure 16 by the cavities on the conic-cylindrical hull ($x_1 = 15$, $R_{b0} = 1.15$, and $R_{b1} = 2.2$) created by a disc cavitator. The same cavitator and hull were tested in Vlasenko and Savchenko [13].

The value $R_{b1} = 2.2$ is smaller than the critical one based on (60); therefore no "jumps" in cavity length (as shown in Figure 15) are expected. At the greater value of the cavitation number $\sigma_0 = 0.167$ the corresponding values of u_1 are negative and ventilation does not increase the cavity length significantly (see Figure 16). On the contrary, at the smaller cavitation number $\sigma_0 = 0.06$ the values of u_1 become positive and the same values of the ventilation rate drastically increase the cavity length (see Figure 16). In the experiments performed in Vlasenko and Savchenko [13] the values of Δ were smaller than 0.0001. The calculations show that the cavity shapes are very close to the vapor ones (shown in Figure 16 by dashed lines) at these small gas injection rates. Thus, the changes in the pressure inside the cavity (or different values of σ_0) are the main reason of changes in the cavity length in the experiments (Vlasenko and Savchenko [13]). Unfortunately, the pressure inside the cavity was not measured in Vlasenko and Savchenko [13].

If at a zero or a small value of Δ the cavity covers a hull, its length approaches the value x_k and $R_b(x) = R_{bk}$ at $x > x_k$ (in particular, for a bounded hull $R_{bk} = 0$), then the value u_k is negative (according to formula (43)). In this case the cavity length depends on the ventilation rate very slightly. This fact

was revealed also in experiments (see Wosnik et al. [10] and Vlasenko and Savchenko [13]).

9. Asymptotic Solution at Small Values of the Ventilation Rate

9.1. Basic Equations. If the gas injection rate is small enough $Q(t) \ll 1$, the solution of the nonlinear equation (17) can be expressed as follows:

$$R^2(x,t) \approx R^2_{(0)}(x,t) + R^2_{(1)}(x,t),$$
$$R^2_{(0)}(x,t) \gg R^2_{(1)}(x,t), \tag{61}$$

where $R_{(0)}(x,t)$ is the solution of (17) at zero ventilation rate $Q(t) = 0$,

$$\varepsilon^2 \ln \varepsilon Z(A_0) + \varepsilon^2 \left[Z(A_0) \ln F_0 + Z(B_0) + 0.5 A_0^2 F_0^{-2} \right] = 0.5\sigma_0(t) \pm x \mathrm{Fr}^{-2}(t), \tag{62}$$

$$A_0(x,t) = F_0(x,t) \left(\frac{\partial F_0}{\partial x} + \tau \frac{\partial F_0}{\partial t} \right);$$
$$F_0^2(x,t) = \frac{R^2_{(0)}(x,t)}{\varepsilon^2};$$
$$B_0(x,t) = -A_0(x,t) \ln 2 - \frac{1}{2} \int \frac{\partial A_0(\xi,t)}{\partial \xi} \operatorname{sign}(x-\xi) \ln |x-\xi| \, d\xi. \tag{63}$$

Function $R_{(1)}(x,t)$ is a solution of the following equations:

$$\varepsilon^2 \ln \varepsilon Z(A_1) = \frac{\rho_g \tau(t)}{\pi\rho} \frac{\partial}{\partial t} \left[Q(t) \int_0^x \frac{dx}{W_0(x,t)} \right] + \frac{\rho_g Q(t) S(t)}{\pi\rho} \int_0^x \frac{dx}{W_0(x,t)} - \frac{\rho_g Q^2(t)}{2\rho\pi^2} \left[W_0^{-2}(0,t) - W_0^{-2}(x,t) \right], \tag{64}$$

$$W_0(x,t) = R^2_{(0)}(x,t) - R_b^2(x,t), \tag{65}$$

$$A_1(x,t) = F_1(x,t) \left(\frac{\partial F_1}{\partial x} + \tau \frac{\partial F_1}{\partial t} \right);$$
$$F_1^2(x,t) = \frac{R^2_{(1)}(x,t)}{\varepsilon^2}. \tag{66}$$

To solve the nonlinear integral-differential equation (62) the asymptotic series obtained in Nesteruk [30] and the standard initial and boundary conditions (19) can be used for the function $R_{(0)}(x,t)$. If the accuracy restrictions are not very severe, the first approximation equation (similar to (9) or (10) with main terms of order $\varepsilon^2 \ln \varepsilon$ only) can be easily solved. Knowing the function $R_{(0)}(x,t)$ the right hand part of (64) and (65) can be calculated and the function $R_{(1)}(x,t)$ can be determined as a solution of the set of linear differential equations with the partial derivatives (64) and (66) and zero initial and boundary conditions. Thus the presentation (61) allows avoiding the nonlinear integral-differential equations.

9.2. Stability of the Steady Ventilated Cavities. Let us use the main term $R_{(0)}(x,t)$ in (61) and the first approximation in (62) to analyze the stability of ventilated cavities at small values of the gas injection rates. Let us consider the steady cavity with a constant gas pressure inside the cavity p_0. According to the first approximation of (62) the cavity radius $R_0(x) \approx R_{(0)}(x)$ is given by formula (27). Let us consider small changes in gas pressure $\Delta p = p - p_0$, where p is a new constant gas pressure inside the cavity. According to (27) and (1) the new cavity radius can be written as follows:

$$R^2(x) = \frac{\sigma_0 x^2}{2 \ln \varepsilon} - \frac{\Delta p x^2}{\rho U_\infty^2 \ln \varepsilon} \pm \frac{x^3}{3\mathrm{Fr}^2 \ln \varepsilon} + 2\beta x + 1. \tag{67}$$

Here we neglect the changes in the vapor pressure.

Integration of formulas (27) and (67) allows calculating the changes in the cavity volume ΔG_1:

$$\Delta G_1 \approx -\frac{\Delta p \pi L_0^3}{3\rho U_\infty^2 \ln \varepsilon}, \tag{68}$$

where L_0 is the initial cavity length, which is measured along the axis x and can be found from (27) as follows:

$$R_b^2(L_0) = \frac{\sigma_0 L_0^2}{2 \ln \varepsilon} \pm \frac{L_0^3}{3\mathrm{Fr}^2 \ln \varepsilon} + 2\beta L_0 + 1. \tag{69}$$

Here we suppose the body radius $R_b(x)$ to be time independent; therefore ΔG_1 yields also the changes in the volume of gas.

On the other hand for a fixed mass of gas its pressure and volume G are related according to the polytropic relationship:

$$pG^\gamma = p_0 G_0^\gamma, \tag{70}$$

where $\gamma = \text{const}$ (in particular, for isothermal process $\gamma = 1$); the initial volume of gas can be calculated with the use of (27) as follows:

$$G_0 = \pi \left[\frac{\sigma_0 L_0^3}{6 \ln \varepsilon} \pm \frac{L_0^4}{12\mathrm{Fr}^2 \ln \varepsilon} + \beta L_0^2 + L_0 - \int_0^{L_0} R_b^2(x)\, dx \right]. \tag{71}$$

Putting in (70) $p = p_0 + \Delta p$ and $G = G_0 + \Delta G_2$ and linearization yield

$$\Delta G_2 \approx -\frac{\Delta p G_0}{\gamma p_0}. \tag{72}$$

Values ΔG_1 and ΔG_2 have opposite signs (see (68) and (72)) and can compensate each other, if $|\Delta G_2| > |\Delta G_1|$. Otherwise the cavity becomes unstable. The critical value of the gas pressure can be obtained from $|\Delta G_2| = |\Delta G_1|$, (68), and (72):

$$p_0^{(\mathrm{cr})} = -\frac{3 G_0 \rho U_\infty^2 \ln \varepsilon}{\gamma \pi L_0^3}. \tag{73}$$

At smaller values of the gas pressure the cavity is stable. If $p_0 > p_0^{(cr)}$, the cavity becomes unstable. The existence of the critical gas pressure value was revealed in experiments (e.g., Michele [20]) and supported by the theory developed by Paryshev [23, 24].

Equation (73) can be rewritten in the dimensionless form taking into account the definition of the cavitation number (1):

$$\sigma_v = \sigma_0^{(cr)} - \frac{6G_0 \ln \varepsilon}{\gamma \pi L_0^3}, \tag{74}$$

where the vapor cavitation number

$$\sigma_v = \frac{2\left(p_\infty - p_v\right)}{\rho U_\infty^2} \tag{75}$$

and the critical value of the cavitation number can be obtained from (69) as follows:

$$\sigma_0^{(cr)} = \frac{2\ln\varepsilon}{L_0^2}\left[R_b^2\left(L_0\right) \mp \frac{L_0^3}{3\mathrm{Fr}^2 \ln\varepsilon} - 2\beta L_0 - 1\right]. \tag{76}$$

It follows from (71), (73), and (76) that

$$\sigma_v = \frac{2\left(\gamma - 1\right)\ln\varepsilon}{\gamma L_0^2}\left[R_b^2\left(L_0\right) \mp \frac{L_0^3}{3\mathrm{Fr}^2 \ln\varepsilon} - 2\beta L_0 - 1\right] - \frac{6\ln\varepsilon}{\gamma L_0^3}\left[\beta L_0^2 + L_0 \pm \frac{L_0^4}{12\mathrm{Fr}^2 \ln\varepsilon} - \int_0^{L_0} R_b^2(x)\,dx\right]. \tag{77}$$

Formula (77) allows calculating the critical value of σ_v for every value of the cavity length. The corresponding critical cavitation number can be calculated with the use of (76). Thus the dependence $\sigma_0^{(cr)}(\sigma_v)$ can be obtained. In particular, for an empty isothermal cavity at large Froude numbers ($R_b \equiv 0$, $\gamma = 1$, and $\mathrm{Fr} \to \infty$) it follows from (77) and (76) that

$$\sigma_v = -\frac{6\left(\beta L_0 + 1\right)\ln\varepsilon}{L_0^2}, \qquad \sigma_0^{(cr)} = -\frac{2\left(2\beta L_0 + 1\right)\ln\varepsilon}{L_0^2}. \tag{78}$$

Examples of calculations based on (78) are presented in Figure 17. Stable cavities correspond to regions located above the corresponding curves. In the case of the slender cavitators, the function $\sigma_0^{(cr)}(\sigma_v)$ depends on β in comparison with the relationship

$$\frac{\sigma_0^{(cr)}}{\sigma_v} \approx 0.37 \tag{79}$$

obtained by Paryshev [23] for the isothermal cavities created by nonslender cavitators with the use of semiempirical formulas for the cavity shape. In the cases of long cavities ($L_0 \to \infty$) and for the base cavities with $\beta = 0$ the relationships (78) yield the formulas

$$\frac{\sigma_0^{(cr)}}{\sigma_v} \approx \frac{2}{3}; \qquad \frac{\sigma_0^{(cr)}}{\sigma_v} \approx \frac{1}{3}, \tag{80}$$

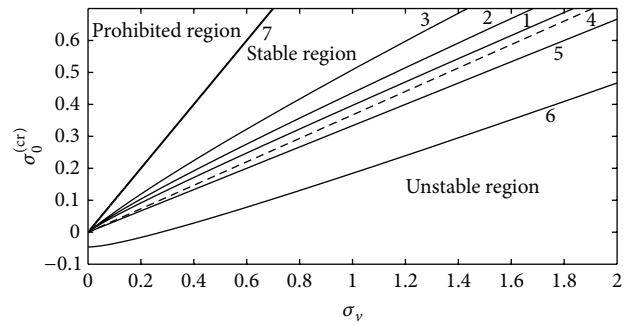

Figure 17: The dependences $\sigma_0^{(cr)}(\sigma_v)$ for the empty isothermal cavity ($R_b \equiv 0$ and $\gamma = 1$) at $\mathrm{Fr} \to \infty$. Curves 1–3 correspond to the cavities, created by conical cavitators with $\beta = 0.05$, 0.1, and 0.273, respectively; $\varepsilon = \beta$. Paryshev's theoretical linear dependence (79) is represented by dashed line 4. Base cavities for $\beta = 0, -0.1$ are represented by curves 5 and 6, respectively ($\varepsilon = 0.1$). The restriction $\sigma_0^{(cr)} = \sigma_v$ is shown by the bold line 7.

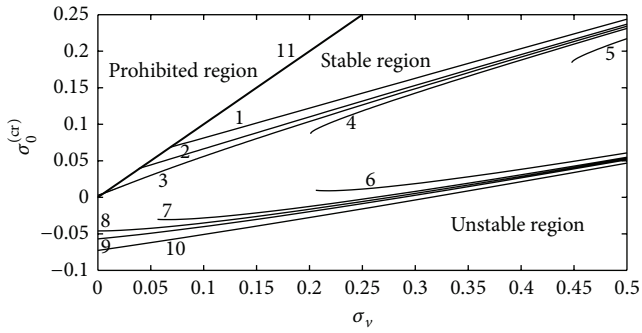

Figure 18: The dependences $\sigma_0^{(cr)}(\sigma_v)$ for the empty isothermal cavity ($R_b \equiv 0$, $\gamma = 1$, and $\varepsilon = 0.1$) at different values of the Froude number. Curves 1–5 correspond to the cavities, created by the conical cavitator ($\beta = 0.1$), and curves 6–10 correspond to base cavities ($\beta = -0.1$). The direction of the flow coincides with the direction of the gravity for the curves 1, 2, 9, and 10 and is opposite for the curves 4–7. The cases $\mathrm{Fr} \to \infty$ are shown by lines 3 and 8; $\mathrm{Fr} = 5$ corresponds to lines 1, 5, 6, and 10; $\mathrm{Fr} = 10$ corresponds to lines 2, 4, 7, and 9. The restriction $\sigma_0^{(cr)} = \sigma_v$ is shown by the bold line 11.

respectively. The difference between the first relationships (80) and (79) can be explained by the limited accuracy of both the first approximation equation (27) and the semiempirical formulas used by Paryshev. In the experiments with 2D cavities the value $\sigma_0^{(cr)}/\sigma_v \approx 0.2$ was measured by Michel [20]. It can be seen from Figure 17 that the largest stability regions correspond to the base cavities ($\beta \le 0$). In particular, stable cavities with negative cavitation number are possible at $\beta < 0$. It follows from (78) that the cavitation number is limited by value $2\beta^2 \ln\varepsilon$, obtained in Nesteruk [32].

The influence of the gravity forces is shown in Figure 18. For the conical cavitators the presence of gravity diminishes the stability regions, if its direction coincides with the direction of the ambient flow (see curves 1 and 2). In particular, there are no stable cavities at some small values of σ_v. Opposite behaviour is typical for the base cavities (see curves 9 and 10). If the directions of the ambient flow and

the gravity are opposite the minimal cavitation number exists (this fact was already discussed in Section 6). The critical cavity shapes are similar to the solid line shown in Figure 4. For such lines $dL/d\sigma_0 \to \infty$; therefore the minimum values of the cavitation number can be calculated from (76) with the use of the condition $d\sigma_0/dL_0 = 0$. These minimum possible values of the cavitation number correspond to the ends of the curves 4–7 (see Figure 18) and yield additional stability restrictions.

The cavities with the hulls located inside have smaller stability regions in comparison with the empty cavities (due to the smaller value of G_0 (see (73)). The same conclusion has been drawn out by Paryshev [23]. To illustrate this fact, let us take the neutral hull shape:

$$R_b^2(x) = \frac{\sigma_0 x^2}{2\ln\varepsilon} \pm \frac{x^3}{3\mathrm{Fr}^2\ln\varepsilon} + 2\beta x + R_{b0}^2. \tag{81}$$

For such hull formula (27) is a solution of (20) at any value of the gas injection rate; that is, (27) is not only the approximation of the steady cavity shape at a small ventilation but also the exact solution at any gas injection rate. If $\mathrm{Fr} \to \infty$, (81) coincides with the relationship (53). The length of the neutral hull L_b can be obtained from (81) as a solution of $R_b^2(L_b) = 0$. Let us assume that $R_b^2 \equiv 0$ at $x > L_b$. Then $R_b^2(L_0) = 0$ and for the isothermal gas processes inside the cavity, (77) can be rewritten as follows:

$$\sigma_v = -\frac{6\ln\varepsilon}{L_0^3}\left[\beta\left(L_0^2 - \frac{1}{3}L_b^2\right) + L_0 - \frac{2}{3}L_b R_{b0}^2 \pm \frac{L_0^4 + L_b^4/3}{12\mathrm{Fr}^2\ln\varepsilon}\right]. \tag{82}$$

Let us consider at first the case of very small area of the circular channel between the cavity and the hull surface $R_{b0} \to 1$. Then $L_b \to L_0$ and formulas (82) and (76) yield

$$\sigma_v \approx -\frac{2\ln\varepsilon}{L_0^2}\left[2\beta L_0 + 1 \pm \frac{L_0^3}{3\mathrm{Fr}^2\ln\varepsilon}\right] = \sigma_0^{(\mathrm{cr})}. \tag{83}$$

Therefore, cavities with the very small area of the circular channel between the cavity and the hull can be stable at the cavitation numbers which are very close to maximum possible value, σ_v. Thus such cavities are mostly unstable.

Let us consider the case of the maximal area of the circular channel, that is, $R_{b0} \to 0$. For the base cavities ($\beta \le 0$ and $R_{b0} \to 0$) the hull volume tends to zero. The stability of the empty base cavities has been already investigated before and illustrated in Figures 17 and 18. It can be seen that the stability regions are rather large. In the case $\beta > 0$ and $R_{b0} \to 0$, the corresponding cavities are not empty. Let us investigate their stability at $\mathrm{Fr} \to \infty$. It follows from (76) and (81) that

$$L_b = -\frac{4\beta\ln\varepsilon}{\sigma_0} = \frac{2\beta L_0^2}{2\beta L_0 + 1}. \tag{84}$$

Substituting (84) into (82) yields that at fixed value of $\sigma_0^{(\mathrm{cr})}$ the corresponding value of σ_v is smaller by the value $\Delta\sigma_v = 8\beta^2 L_0 \ln\varepsilon/(2\beta L_0 + 1)^2$; therefore the corresponding stability regions are smaller in comparison with the case of empty cavities (shown in Figure 17 by curves 1–3). The examples of calculations based on (78), (81), and (82) are shown in Figure 19. It can be seen that grater values of the volume of the hull part located inside the cavity (larger values of L_b/L_0) decrease the stability region. The most stable are the empty cavities presented in Figure 19 by dashed lines 7 and 8.

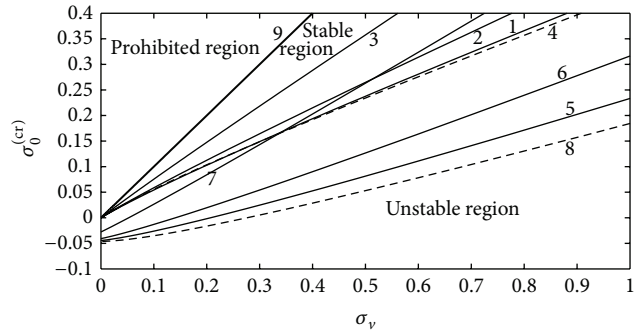

FIGURE 19: The dependences $\sigma_0^{(\mathrm{cr})}(\sigma_v)$ for the isothermal cavity ($\gamma = 1$) on the neutral shaped hull (81) at $\mathrm{Fr} \to \infty$ and $\varepsilon = 0.1$. Curves 1–4 correspond to $\beta = 0.1$ and curves 5–8 correspond to $\beta = -0.1$. Solid lines 1–3 and 5–7 correspond to the values $L_b/L_0 = 0.5$, 0.7, and 0.9, respectively. For comparison the cases of the empty cavity are shown by dashed lines 4 and 8. The restriction $\sigma_0^{(\mathrm{cr})} = \sigma_v$ is shown by the bold line 9.

It must be noted that the experiments at standard room temperature and at values of the pressure close to the atmospheric one yield rather grate values of σ_v (e.g., $\sigma_v > 2$ at $U_\infty < 10$ m/s). At these values of σ_v the corresponding critical cavitation number is rather large and cavity length is rather small. Thus, it is difficult to obtain long stable empty cavities in the low speed experiments. Vlasenko and Savchenko [13] revealed stable cavities closing on the conical part of the hulls. Their length is restricted by the value $L_0 \approx 9$, obtained at some gas injection rate for the hull shown in Figure 16. Further increasing of the ventilation leads to the drastic increase of the cavity length. Since the values of gas injection rate are too small to change the cavity shape significantly, such behaviour can be treated as a loose of stability.

Let us try to estimate σ_v corresponding to the experimental critical value $L_0 = 9$ with the use of (77) and compare with the experimental value $\sigma_v \approx 2.52$ (Vlasenko and Savchenko [13]). Since the experiments were performed for the disc cavitator, we need to use formula (29) for the initial part of the cavity at $x < 2$ and take into account the corresponding volume of the gas $\Delta G_0 = \pi[0.2(7^{5/3} - 1) - 2]$. We assume that $R_b = 1$ at $x < 2$, $\varepsilon = \beta = 0.273$, $\gamma = 1$, and $\mathrm{Fr} \to \infty$. The calculations based on the modified formula (77) yield $\sigma_v \approx 2.54$ which is very close to the experimental value.

The obtained results can also be applied for the separated bubbles. In incompressible liquid $\gamma \to \infty$ and according to (72) such bubble is always unstable. In the case of a gas, the same gas is present in the external flow and inside the separated zone (there is no more a huge difference in densities as for a gas cavity located in the water flow). Nevertheless, the small velocities inside the separated zone allow supposing the pressure to be constant and using the developed theory.

In this case the vapor cavitation number coincides with the Euler number as follows:

$$\sigma_v = \mathrm{Eu} = \frac{2p_\infty}{\rho_g U_\infty^2}. \tag{85}$$

According to the presented analysis, is difficult to obtain long enough stable separated bubbles for Eu $>$ 2, but at smaller values of the Euler number the separated zones can be stable. Therefore, the Euler number must be taken into account in simulations of the gas flow separation (as mentioned in Nesteruk [25]).

9.3. Stability of the Pulsating Ventilated Cavities. In the previous section it was shown that steady stable cavities at low speeds (U_∞ $<$ 10 m/s) have to be very short. In order to cover long hulls it is possible to use pulsating cavities which were investigated experimentally in Silberman and Song [18], Song [19], Michel [20], and Zou et al. [21] and by many other authors. The theories of such empty cavities were proposed by Woods [22], Paryshev [23, 24], Nesteruk [25], and Semenenko [26]. Here we consider the small oscillations of the pressure inside the cavity which covers the hull.

Let us suppose that the gas injection rates are small enough to use only the main term $R_{(0)}(x,t)$ in (61) and to consider the pressure inside the cavity to be only time dependent. The corresponding changes of the cavitation number can be represented as follows:

$$\sigma_0(t) = \overline{\sigma}_0 + b_1 \sin(2\pi t), \tag{86}$$

where $\overline{\sigma}_0$ is the average value of the cavitation number and the dimensionless time is based on the period of oscillations T.

Let us suppose the velocity of the ambient flow and the hull shape to be time independent and use the radius R_0 of the cavity and the body at the cross section of cavity origin $x = 0$ (see Figure 1) for dimensionless lengths and to calculate the parameters (4) and (7). Then

$$\tau = \frac{R_0}{TU_\infty}; \qquad S(t) = 0; \qquad \mathrm{Fr} = \frac{U_\infty}{\sqrt{gR_0}}. \tag{87}$$

Let us take only the main term of order $\varepsilon^2 \ln\varepsilon$ in (62) and use the analytical solution obtained in Nesteruk [28]. In particular, for the harmonic low (86) the following formula was obtained (Nesteruk [33]):

$$R^2(x,t) = \frac{\overline{\sigma}_0 x^2}{2\ln\varepsilon} \pm \frac{x^3}{3\mathrm{Fr}^2\ln\varepsilon} + 2\beta x + 1 + b_2 F_2(x,t), \tag{88}$$

$$F_2(x,t) = 2\pi x\tau\cos[2\pi(t - x\tau)] + \sin[2\pi(t - x\tau)] - \sin(2\pi t);$$

$$b_2 = \frac{b_1}{4\pi^2\tau^2\ln\varepsilon}. \tag{89}$$

Formula (88) shows that for the pulsating cavity $R^2(x,t)$ differs from $R^2(x)$ corresponding to the steady cavity at the mean value of the cavitation number $\overline{\sigma}_0$ by function $b_2F_2(x,t)$. Formula (89) corresponds to a propagating wave with the amplitude increasing downstream. The length of the wave—the minimal distance between maxima or minima of the function (89)—is equal to $1/\tau$. The same behaviour was revealed in experiments (Song [19]).

Integration of (88) allows calculating the cavity volume:

$$G(t) = \pi\int_o^{L(t)} R^2(x,t)\,dx = \pi L\left[\frac{\overline{\sigma}_0 L^2}{6\ln\varepsilon} \pm \frac{L^3}{12\mathrm{Fr}^2\ln\varepsilon} + \beta L + 1\right] + b_3\left[F_3(L,t) - F_3(0,t)\right], \tag{90}$$

$$F_3(s,t) = \frac{\cos[2\pi(t - s\tau)]}{(\pi\tau)} - s\{\sin[2\pi(t - s\tau)] + \sin(2\pi t)\}; \tag{91}$$

$$b_3 = \frac{b_1}{4\pi\tau^2\ln\varepsilon},$$

where the cavity length $L(t)$ may be obtained from

$$R_b^2(L) = \frac{\overline{\sigma}_0 L^2}{2\ln\varepsilon} \pm \frac{L^3}{3\mathrm{Fr}^2\ln\varepsilon} + 2\beta L + 1 + b_2 F_2(L,t). \tag{92}$$

At small values of b_1 (or b_2) the difference between $L(t)$ and the length $\overline{L}$ of the steady cavity at the cavitation number $\overline{\sigma}_0$ must be small, since $\overline{L}$ is a solution of (92) at $b_1 = b_2 = 0$. Here we do not take into account the cases of discontinuous changes in the cavity length discussed in Section 8.5 and shown in Figure 15.

By putting $\Delta L = L - \overline{L}$ into (90) the pulsations of the cavity volume can be calculated:

$$\Delta G(t) = G(t) - \overline{G} \approx b_3\left[F_3\left(\overline{L},t\right) - F_3(0,t)\right], \tag{93}$$

where $\overline{G}$ is the average volume of the steady cavity at the cavitation number $\overline{\sigma}_0$ and can be obtained from (90) at $b_1 = b_3 = 0$. With the use of (93) the average value of the cavity volume pulsations can be calculated:

$$\Delta\overline{G} = \int_o^1 \Delta G(t)\,dt = b_4 F_4\left(\tau\overline{L}\right), \quad b_4 = \frac{b_1}{8\pi^3\tau^3\ln\varepsilon}, \tag{94}$$

$$F_4(y) = \sin[2\pi(1 - y)] - \sin(2\pi y) + \pi y\{\cos[2\pi(1 - y)] - \cos(2\pi y)\}. \tag{95}$$

Equations (94) and (95) show that the average value of the cavity volume pulsations is proportional to the amplitude of the gas pressure pulsations b_1 and can be diminished, when $F_4(y) \approx 0$. It can be expected that the pulsating cavities with zero average value of the volume pulsations are stable; that is, they can exist during a long time. According to the formula (95) the zero values of F_4 are possible at

$$\tau\overline{L} = \frac{\overline{L}'}{T'U'_\infty} = \mathrm{Sh} = n; \quad n = 1, 2, 3, \ldots. \tag{96}$$

Equation (96) shows that stable oscillating cavities occur only at integer values of the Strouhal number Sh or at integer number of waves located on the average cavity length. This fact was revealed in experiments on empty 2D cavities (Song [19]) and supported by the theories developed by Woods [22] and Semenenko [26] for 2D cavities and by Paryshev [23, 24] and Nesteruk [25] for the axisymmetric empty cavities. Presented analysis illustrates that the same behaviour is typical also in the case of rigid hulls located inside the cavity. If the average cavity length is fixed, the corresponding frequencies of pulsations in the cavity and in its wake are limited by (96).

Formula (96) can also be applied for the separation bubbles both in gases and in liquids. In particular, let us compare (96) with the experimental Strouhal numbers for Karman vortex street, measured for circular cylinders of diameter d' at large Reynolds numbers (see, e.g., Theodore von Kármán [38]):

$$\mathrm{Sh}_K = \frac{d'}{T'U'_\infty} \approx 0.2. \tag{97}$$

Since the cylinder diameter d' is few times smaller than the average length of its separated zone, formulas (96) and (97) are in good agreement.

In order to investigate the influence of the ventilation rate on the pulsating cavities, (64) must be solved. But some conclusions can be drawn out with the use of simple physical considerations. At the local minima of the circular channel area the pressure in gas flow and cavity radius decrease and in maxima the pressure in gas flow and cavity radius increase. It leads to the increasing of the pulsation amplitude with the increasing of the ventilation rate. This fact was revealed by experiments (see, e.g., Silberman and Song [18]).

10. Conclusions

The integral-differential equation was obtained to simulate unsteady evolutions of the slender axisymmetric ventilated supercavity with the use of one-dimensional inviscid flow of the incompressible gas in the channel between the cavity surface and the body of revolution. For small ventilation rates, a solution was expressed as asymptotic series. In steady case the nonlinear differential equation and its solutions were obtained. It was shown that the cavity shape depends strongly on the values of the ventilation rate and the cavitation number.

The ventilation can strongly increase and decrease the cavity dimensions. In particular, for the cavities created by the slender conical cavitator the increase of the ventilation rate increases the cavity dimensions. The cavity could become unbounded at some critical values of the ventilation rate. On the other hand, the ventilation can strongly decrease the base cavity length. Some specific neutral hulls ensure no changes in the cavity shape at any value of the ventilation.

Examples of the steady cavity shape calculations for different hulls are presented. It was shown that the cavities can have classical elliptical shapes and be also conical, hyperbolic, and cylindrical. They may also have the minimum of the radius. Peculiarities of the cavity closing near the hull contour discontinuities were investigated.

Simple stability theories for the steady and pulsating cavities at small ventilation rates were proposed. The results are in good agreement with the known theoretical and experimental findings of other authors and generalize them for the cases of the hull, located inside the cavity, and different cavitators and take into account the influence of the gravity. In particular, it was shown that the cavities with a very small area of the circular gas channel between the hull and the cavity surface are unstable and that gravity and the cavitator shape strongly influence the stability. The fact that stable pulsating cavities are possible, when an integer number of waves are located on the average cavity length, is also valid for nonempty cavities.

More complicated models are necessary to simulate the gas flow inside the cavity. In particular, the viscosity of gas has to be taken into account.

Conflict of Interests

The author declares that there is no conflict of interests regarding the publication of this paper.

References

[1] G. V. Logvinovich, *Hydrodynamics of Flows With Free Boundaries*, Naukova Dumka Publishing House, Kiev, Ukraine, 1969.

[2] L. A. Epshtein, *Methods of Theory of Dimensionality and Similarity in Problems of Ship Hydromechanics*, Sudostroenie Publishing House, Leningrad, Russia, 1970, Russian.

[3] L. A. Epshtein, "Characteristics of ventilated cavities and some scale effects, unsteady water flow with high velocities," in *Proceedings of International Symposium IUTAM*, Nauka Publishing House, Moscow, Russia, 1973.

[4] L. A. Epshtein, "On mechanism of pulse processes in end zone of attached cavities," in *Proceedings of the Symposia on Physics of Acoustic-Hydrodynamic Phenomena*, Nauka Publishing House, Moscow, Russia, 1975, Russian.

[5] R. T. Knapp, J. W. Daily, and F. G. Hammitt, *Cavitation*, McGraw-Hill, 1970.

[6] I. T. Yegorov, Y. M. Sadovnikov, I. I. Isayev, and M. A. Basin, *Artificial Cavitation*, Sudostroenie Publishing House, Leningrad, Russia, 1971, Russian.

[7] Y. L. Levkovsky, *Structure of Cavitation Flows*, Sudostroenie Publishing House, Leningrad, Russia, 1978, Russian.

[8] R. Kuklinski, C. Henoch, and J. Castano, "Experimental study of ventilated cavities on dynamic test model," in *Proceedings of the International Symposium on Cavitation (CAV '01)*, Pasadena, Calif, USA, 2001.

[9] J. H. Spurk, "A theory for the gas loss from ventilated cavities," in *Proceedings of the International Summer Scientific School High Speed Hydrodynamics*, pp. 191–195, Cheboksary, Russia, 2002.

[10] M. Wosnik, T. J. Schauer, and R. E. A. Arndt, "Experimental study of a ventilated supercavitating vehicle," in *Proceedings of the International Symposium on Cavitation (CAV '03)*, Osaka, Japan, 2003.

[11] Y. F. Zhuravlev and A. V. Varyukhin, "Numerical simulationof interaction gas jets flowing into water cavity with its free

surfaces simulation," in *Proceedings of the International Conference SuperFAST*, Saint-Petersburg, Russia, 2008.

[12] K. I. Matveev, T. J. Burnett, and A. E. Ockfen, "Study of air-ventilated cavity under model hull on water surface," *Ocean Engineering*, vol. 36, no. 12-13, pp. 930–940, 2009.

[13] Y. D. Vlasenko and G. Y. Savchenko, "Study of the parameters of a ventilated supercavity closed on a cylindrical body," in *Supercavitation*, I. Nesteruk, Ed., pp. 201–214, Springer, 2012.

[14] I. Nesteruk, "Drag effectiveness of supercavitating underwater hulls," in *Supercavitation*, I. Nesteruk, Ed., pp. 79–106, Springer, 2012.

[15] Z. I. Manova, I. Nesteruk, and B. D. Shepetyuk, "Estimations of intensive ventilation influence on the slender axisymmetric cavity shape," *Applied Hydromechanics*, vol. 13, no. 2, pp. 44–50, 2011.

[16] I. Nesteruk and B. D. Shepetyuk, "Shape of artificial axisymmetric cavities at sub- and supercritical values of the ventilation rate," *Applied Hydromechanics*, vol. 14, no. 2, pp. 53–60, 2012 (Ukrainian).

[17] I. Nesteruk and B. D. Shepetyuk, "Shape peculiarities of the base artificial axisymmetric cavities," *Applied Hydromechanics*, vol. 13, no. 3, pp. 69–75, 2011 (Ukrainian).

[18] E. Silberman and C. S. Song, "Instability of ventilated cavities," *Journal of Ship Research*, vol. 5, no. 1, pp. 13–33, 1961.

[19] C. S. Song, "Pulsation of ventilated cavities," *Journal of Ship Research*, vol. 5, no. 4, pp. 8–19, 1962.

[20] J. M. Michel, "Some features of water Flows with Ventilated Cavities," *Journal of Fluids Engineering, Transactions of the ASME*, vol. 106, no. 3, pp. 319–326, 1984.

[21] W. Zou, K.-P. Yu, R. E. A. Arndt, E. Kawakami, and G. Zhang, "On the stability of supercavity with angle of attack," in *Proceedings of the International Symposium on Cavitation (CAV '12)*, Singapore, 2012.

[22] L. C. Woods, "Instability of ventilated cavities," *Journal of Ship Research*, vol. 5, pp. 13–33, 1966.

[23] E. V. Paryshev, "Theoretical investigation of stability and pulsations of axisymmetric cavities," *Trudy TsAGI*, pp. 17–40, 1978.

[24] E. V. Paryshev, "Some Issues of Supercavitating Flow Analysis," in *International Conference SuperFAST*, Saint-Petersburg, Russia, 2008.

[25] I. Nesteruk, "Euler number and flows with boundary-layer separation," in *Theoretical and Experimental Investigations of Some Problems of Aero- and Hydrodynamics*, pp. 66–69, Moscow Institute of Physics and Technology, 1990, Russian.

[26] V. N. Semenenko, "Instability of a plane ventilated supercavity in an infinite stream," *International Journal of Fluid Mechanics Research*, vol. 23, no. 1-2, pp. 134–143, 1996.

[27] J. D. Cole, *Perturbation Methods in Applied Mathematics*, Blaisdell Publishing Company, London, UK, 1968.

[28] I. Nesteruk, "On the shape of a slender axisymmetric nonstationary cavity," *Izvestija AN SSSR*, vol. 4, pp. 39–47, 1980 (Russian), English translation: Fluid Dynamics, volume 15, issue 4, pp. 504-511.

[29] I. Nesteruk, "Influence of the flow unsteadiness, compressibility and capillarity on long axisymmetric cavities," in *Proceedings of the International Symposium on Cavitation (CAV '03)*, Osaka, Japan, 2003.

[30] I. Nesteruk, "Determination of the form of a thin axisymmetric cavity on the basis of an integrodifferential equation," *Fluid Dynamics*, vol. 20, no. 5, pp. 735–741, 1985.

[31] V. N. Semenenko and Y. I. Naumova, "Study of the supercavitating body dynamics," in *Supercavitation*, I. Nesteruk, Ed., pp. 147–176, Springer, 2012.

[32] I. Nesteruk, "On the shape of a slender axisymmetric cavity in a ponderable liquid," *Izvestija AN SSSR*, vol. 6, pp. 133–136, 1979 (Russian), English translation: Fluid Dynamics, volume 14, issue 6, pp. 923-927.

[33] I. Nesteruk, "Some problems of axisymmetric cavitation flows," *Izvestija AN SSSR*, vol. 1, pp. 28–34, 1982 (Russian), English translation: Fluid Dynamics, volume 17, issue 1, pp. 21-27.

[34] I. Nesteruk, "Drag reduction in high-speed hydrodynamics: supercavitation or unseparated shapes," in *Proceedings of the 6th International Symposium on Cavitation (CAV '06)*, Wageningen, The Netherlands, 2006.

[35] I. Nesteruk, "The restrictions of the parameters of cavitational flow," *Applied Mathematics and Mechanics*, vol. 50, pp. 584–588, 1986 (Russian), English translation: Pmm Journal of Applied Mathematics and Mechanics, volume 50, issue 4, pp. 446-449.

[36] I. Nesteruk, "Partial cavitation on slender bodies," *Convex and Concave Cavities, Applied Hydromechanics*, vol. 6, no. 783, pp. 64–75, 2004 (Ukrainian).

[37] A. N. Varghese, J. S. Uhlman, and I. N. Kirschner, "High-speed bodies in partially cavitating axisymmetric flow," in *Proceedings of the International Symposium on Cavitation (CAV '03)*, Osaka, Japan, 2003.

[38] Theodore von Kármán, *Aerodynamics*, McGraw-Hill, 1963.

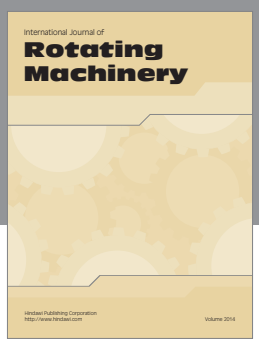

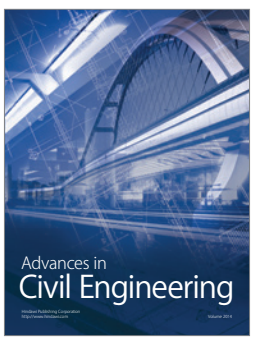

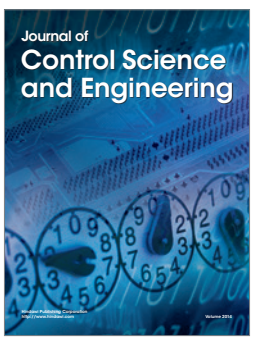

Hindawi
Submit your manuscripts at
http://www.hindawi.com